Open Research Online

The Open University's repository of research publications
and other research outputs

A permethrin metabolite is associated with adaptive immune responses in Gulf War Illness

Journal Item

For guidance on citations see FAQs.

Version: Version of Record

oro.open.ac.uk

A permethrin metabolite is associated with adaptive immune responses in Gulf War Illness

Utsav Joshi[a,b,c], Andrew Pearson[a,b,c], James E. Evans[a,c], Heather Langlois[a,c], Nicole Saltiel[a,c], Joseph Ojo[a,b,c], Nancy Klimas[d,e], Kimberly Sullivan[f], Andrew P. Keegan[a], Sarah Oberlin[a,c], Teresa Darcey[a,c], Adam Cseresznye[a,c], Balaram Raya[a,c], Daniel Paris[a,b,c], Bruce Hammock[g], Natalia Vasylieva[g], Surat Hongsibsong[h], Lawrence J. Stern[i,j], Fiona Crawford[a,b,c], Michael Mullan[a,b,c], Laila Abdullah[a,b,c,*]

[a] Roskamp Institute, 2040 Whitfield Ave, Sarasota, FL, USA
[b] Open University, Milton Keynes, UK
[c] James A. Haley VA Hospital, Tampa, FL, USA
[d] NOVA Southeastern University, Ft. Lauderdale, FL, USA
[e] Miami VAMC, Miami, FL, USA
[f] Boston University School of Public Health, Boston, MA, USA
[g] Department of Entomology and Nematology, UCD Comprehensive Cancer Center, University of California Davis, Davis, CA, USA
[h] Environment and Health Research Unit, Research Institute for Health Science, Chiang Mai University, Chiang, Thailand
[i] Department of Biochemistry and Molecular Pharmacology, University of Massachusetts Medical School, Worcester, MA, USA
[j] Department of Pathology, University of Massachusetts Medical School, Worcester, MA, USA

ARTICLE INFO

ABSTRACT

Gulf War Illness (GWI), affecting 30% of veterans from the 1991 Gulf War (GW), is a multi-symptom illness with features similar to those of patients with autoimmune diseases. The objective of the current work is to determine if exposure to GW-related pesticides, such as permethrin (PER), activates peripheral and central nervous system (CNS) adaptive immune responses. In the current study, we focused on a PER metabolite, 3-phenoxybenzoic acid (3-PBA), as this is a common metabolite previously shown to form adducts with endogenous proteins. We observed the presence of 3-PBA and 3-PBA modified lysine of protein peptides in the brain, blood and liver of pyridostigmine bromide (PB) and PER (PB + PER) exposed mice at acute and chronic post-exposure timepoints. We tested whether 3-PBA-haptenated albumin (3-PBA-albumin) can activate immune cells since it is known that chemically haptenated proteins can stimulate immune responses. We detected autoantibodies against 3-PBA-albumin in plasma from PB + PER exposed mice and veterans with GWI at chronic post-exposure timepoints. We also observed that *in vitro* treatment of blood with 3-PBA-albumin resulted in the activation of B- and T-helper lymphocytes and that these immune cells were also increased in blood of PB + PER exposed mice and veterans with GWI. These immune changes corresponded with elevated levels of infiltrating monocytes in the brain and blood of PB + PER exposed mice which coincided with alterations in the markers of blood-brain barrier disruption, brain macrophages and neuroinflammation. These studies suggest that pesticide exposure associated with GWI may have resulted in the activation of the peripheral and CNS adaptive immune responses, possibly contributing to an autoimmune-type phenotype in veterans with GWI.

1. Introduction

Gulf War Illness (GWI) affects approximately 30% of the US military personnel who were deployed to the 1991 Gulf War (GW) (White et al., 2016). Nearly 30 years later, GW veterans continue to experience debilitating symptoms such as pain, fatigue and memory problems.

Clinical studies suggest that immune dysfunction and chronic inflammation are among the key causes of the symptoms experienced by ill GW veterans (White et al., 2016). Studies using the rodent models of GWI implicate both the central nervous system (CNS) and peripheral immune system in contributing to the pathogenesis of this illness (Koo et al., 2018). However, a better understanding of these immune

responses in GWI would further contribute towards the development of biomarkers and therapies for the CNS symptoms and pathology of GWI.

While no single etiological factor has been definitively linked to GWI (Binns et al., 2008), reports compiled by the Research Advisory Committee (RAC) on GWI based on self-reported systematic retrospective data collection from GW veterans implicate exposure to GW chemicals, such as an anti-nerve agent pyridostigmine bromide (PB), an irreversible acetylcholinesterase (AChE) inhibitor and pesticides like permethrin (PER), in the pathogenesis of GWI. It is now well established that pesticide exposure played a significant role in the manifestation of GWI (Binns et al., 2008; Sullivan et al., 2018). According to Department of Defense (DoD) reports, 62% of the ground troops reported being exposed to any pesticides (Winkenwerder, 2003). Among these, 44% were pesticide sprays that contained pyrethroids, such as PER (Binns et al., 2008). Exposure to pesticides in humans can be associated with autoimmune disorders (Thrasher et al., 1993). Several case reports documented that acute pyrethroid intoxication in humans is associated with an autoimmune clinical phenotype, including disorders like scleroderma and myasthenia-like syndromes (Müller-Mohnssen, 1999; Proudfoot, 2005; Gangemi et al., 2016). The most compelling evidence for autoimmune abnormalities in GWI comes from studies showing increases in immunoglobulin G (IgG) and T- and B-cells in the blood of veterans with GWI compared to healthy GW veterans (Vojdani and Thrasher, 2004), and is supported by a study showing elevated autoantibodies against brain-specific proteins, such as glial fibrillary acidic protein (GFAP) and tau in blood from veterans with GWI (Abou-Donia et al., 2017).

Low molecular weight chemicals can form adducts with endogenous proteins, and these chemically modified proteins can elicit an adaptive immune response (Warrington, 2012). Studies have shown that a 3-phenoxybenzoic acid (3-PBA) is a common metabolite of PER, which is generated by esterase cleavage followed by enzymatic oxidation (Noort et al., 2008). It is shown that 3-PBA can undergo glucuronidation in the liver for excretion in urine to form 1-O-(3-phenoxybenzoyl)-ß-D-glucopyranuronate (Glu-3-PBA) (Noort et al., 2008). This Glu-3-PBA has been shown to further react to form an amide with lysine in proteins (Noort et al., 2008). Others have shown that chemically-haptenated proteins can reach the lymphatic system where they encounter immune cells that are involved in antigen presentation to T- and B-cells (Karlsson et al., 2018). These studies suggest a role of haptenated proteins in promoting autoimmune responses. As such, an activation of autoimmune responses in GWI could be downstream of PER exposure that occurred during the GW conflict.

Autoantibodies against brain proteins are a part of a continuum of many autoimmune disorders (Diamond et al., 2013). An example of this is Sydenham's chorea, a neurological manifestation of rheumatic fever where peripheral autoantibodies against Group A β-hemolytic streptococcus cross-reacts with neuronal proteins (Diamond et al., 2013). In systemic lupus erythematosus (SLE), peripherally generated anti-DNA antibodies enter the brain and cross-react with N-methyl-D-aspartate (NMDA) receptors (Omdal et al., 2005). In other autoimmune disorders, such as multiple sclerosis (MS), studies suggest that a breach in the blood-brain barrier (BBB) allows CNS proteins to leak into the periphery where immune cells first encounter them. Alternatively, these immune cells can gain antigen experience within the cervical lymph nodes where CNS antigens drain (Stern et al., 2014). While the exact mechanisms behind brain and peripheral immune cross-talk remain unknown in GWI, the presence of autoantibodies against brain proteins and evidence of glia activation in mouse models do suggest an involvement of the immune system in promoting the CNS pathology of GWI (Abdullah et al., 2016; Abou-Donia et al., 2017; Joshi et al., 2018).

Increases in astroglia activation, nuclear factor kappa-B (NFκB) phosphorylation and proinflammatory cytokines are commonly observed in the brains of GWI rodent models (Abdullah et al., 2011, 2012, 2016; Parihar et al., 2013; Zakirova et al., 2015; Joshi et al., 2018). Elevated proinflammatory cytokines can increase matrix metalloproteinase 9 (MMP9) activity at the BBB and enhance the transmigration process, potentially promoting the infiltration of peripheral immune cells into the CNS (Song et al., 2015). Among these, Ly6C+ monocytes are capable of converting to macrophages upon CNS infiltration (Wohleb et al., 2013; Miró-Mur et al., 2016). Increases in C-C chemokine receptor type 2 (CCR2) and its ligand, CCL2, were observed in the brains of a GWI mouse model of combined PB and PER (PB + PER) exposure (Joshi et al., 2018). In neuroinflammatory conditions, CCL2 released by astroglia recruits CCR2-expressing peripheral monocytes into the parenchyma, leading to the activation of NFκB-mediated inflammatory pathways (Gerard and Rollins, 2001; Jimenez et al., 2010; Bose and Cho, 2013; Harrison-Brown, Liu and Banati, 2016; Parillaud et al., 2017). These studies suggest that peripheral adaptive immune responses could be involved in promoting neuroinflammation in GWI.

We hypothesize that exposure to PER results in 3-PBA-haptenation of proteins and that haptenated proteins presented by antigen-presenting cells (APC) could activate T- and B-cells, resulting in autoantibody production. The presence of haptenated proteins in the CNS may promote infiltration of peripheral immune cells, which would further contribute to neuroinflammation. In this study, we determined the presence of 3-PBA modified lysine (3-PBA-Lys) in proteins and 3-PBA recovered from protein hydrolysis in the brains and livers of a PB + PER GWI mouse model. We examined the presence of autoantibodies against 3-PBA-haptenated albumin in plasma from PB + PER exposed mice and in veterans with GWI. We investigated the ability of 3-PBA-haptenated albumin to activate peripheral T- and B-cells and determined that these immune cells are elevated in the blood of PB + PER exposed mice and in veterans with GWI. We determined that proinflammatory monocytes capable of tissue infiltration are present in the blood of PB + PER exposed mice. We also examined infiltrating monocytes and macrophages derived from these monocytes in the brains of PB + PER exposed mice. Collectively, these studies will help determine the role of PER metabolites in activating adaptive immune responses in GWI.

2. Material and methods

2.1. Human subjects

Plasma and/or peripheral blood mononuclear cells (PBMC) were utilized from 3 different cohorts: (1) GWI and GW control veterans recruited at the Roskamp Institute Clinics; (2) GWI cases and GW controls from the Boston Gulf War Illness Consortium (GWIC); and (3) subjects from Thailand who were farm workers or consumed pyrethroid-infested fruits and vegetables and either had positive or negative urine 3-PBA measurements. Plasma from age- and gender-matched GWI and control GW veterans were used for this study. The Kansas GWI criteria (Steele, 2000) were used to diagnose GWI. The Kansas GWI criteria require that GW veterans show symptoms in at least 3 of 6 symptom domains (fatigue/sleep problems, somatic pain, neurological/cognitive/mood symptoms, gastrointestinal symptoms, respiratory symptoms, and skin abnormalities). Study participants were excluded if they reported being diagnosed with another medical condition that could explain their chronic health symptoms. Sample collection at the Roskamp Institute Clinics was approved by the Western Institutional Review Board (WIRB), and all protocols were conducted in accordance with relevant guidelines and regulations. Recruitment of study subjects and blood collection to obtain plasma and PBMC has been described previously (Emmerich et al., 2017; Qiang et al., 2017; Joshi et al., 2018) and demographic details are provided in Table 1A. Subjects were also excluded from the study if they were currently on any steroid medication to minimize interferences from the effects of these medications at the time of the blood draw. Controls were veterans deployed to the 1991 GW who did not meet the Kansas GWI criteria or any of the exclusionary criteria listed above. Plasma and PBMC collection at the Boston GWIC were approved by the Boston University IRB. As described

Table 1A
Demographics of the Gulf War veteran autoantibody cohort.

	Controls (GW veteran)	GWI cases
N total	10	14
Age (Mean ± SEM)	54.3 ± 7.6	52.4 ± 7.5
Male (%)	79.7%	86%
Self-report of pesticide exposure during war	5(50%)	95% (12)
Self-report of PB exposure during war	60% (6)	100% (14)
Ethnicity		
Caucasian	8 (70%)	11 (78.4%)
African American	2 (3%)	2 (14.2%)
Other/Multiracial	-	1 (7.13%)

There was no significant difference in age among two groups.

Table 1B
Demographics of the Gulf War veteran Boston consortium cohort.

	Controls (GW veteran)	GWI cases
N total	12	12
Age (Mean ± SEM)	51.23 ± 8.56	54.3 ± 7.4
Male (%)	83.33%	100%
Self-report of pesticide exposure during war	25% (3)	83.33% (10)
Self-report of PB exposure	83.33% (10)	100% (12)
Ethnicity		
Caucasian	9 (75%)	10 (83.4%)
African American	2 (16.67%)	1 (8.3%)
Other/Multiracial	1 (8.33%)	1 (8.3%)

There was no significant difference in age among two groups.

Table 2
Demographics of the subjects from Thailand.

	Negative Controls (no urine 3PBA detected)	Positive cases (urine3-PBA detected)
N total	5	5
Age (Mean ± SEM)	57.3 ± 7.6	61.4 ± 6.33
Male (%)	80%	80%
Pesticide exposure	20% (1)	66.6% (3)
PB exposure	0	0
Occupation		
Farm worker	60% (3)	60% (3)
Non-farm worker	40% (2)	40% (2)

There was no significant difference in age among two groups.

above, the Kansas GWI criteria (Steele, 2000) were used to diagnose GWI, exclusion criteria are the same as those described for the cohort above. Demographic details for GWIC samples are provided in Table 1B. Self-report of pesticide exposure was based on questions which inquired whether they had worn a uniform saturated with pesticide and/or used pesticide cream/spray. Using these data, a summary variable was generated which assigned yes/no to pesticide exposure. Since the exposure status of GW veterans is based on self-report, we also examined plasma from samples obtained from farm and non-farm workers with documented exposure to pyrethroids and measurements of 3-PBA in urine. These were occupational health worker who were exposed to different pyrethroid pesticides during their occupation, and were used as positive and negative controls for a 3-PBA-albumin autoantibody detection assay. All the participants gave their written consents and the study was approved by their respective IRBs. A detailed demographic table is provided in Table 2. Many of these age- and gender-matched people had been exposed to pyrethroids during their occupation, and half of them had 3-PBA detected in their urine (n = 5 positive and n = 5 negative).

2.2. Animals

All procedures on mice were approved by the Roskamp Institute's Institutional Animal Care and Use Committee (IACUC) and were conducted in compliance with the Office of Laboratory Animal Welfare and laboratory animal care guidelines as previously described (Abdullah et al., 2011; Zakirova et al., 2015). Mice were maintained with a 12 h light/dark cycle in a temperature-controlled environment (21 ± 2 °C). Male C57BL/6 mice (3 months of age, weight 25 g ± 0.7 SD) were co-administered 0.7 mg/kg of pyridostigmine bromide (PB) (Fisher Scientific Hanover Park, IL) and 200 mg/kg of PER (Sigma Aldrich, St. Louis, MO, USA) in a single 50 μL intraperitoneal (i.p.) injection in dimethyl sulfoxide (DMSO) (Sigma Aldrich, St. Louis, MO, USA) or DMSO alone (control) daily for 10 consecutive days. Mice were divided in two groups with the control group receiving vehicle only (DMSO) and the GWI group receiving vehicle along with PB and PER. A timeline of the study procedures is provided as Fig. 1.

2.3. Detection and quantification of 3-PBA using LC/MS reverse-phase analysis:

Levels of 3-PBA in plasma, brain and liver were quantified as described by Ahn et al. (2011). Briefly, 400 mg of liver and 100 mg of brain from both control and PB + PER exposed mice were homogenized in 1 mL of PBS, and a protein crash was then performed via the addition of 4 mL of acetone. Samples were then subjected to acid hydrolysis by
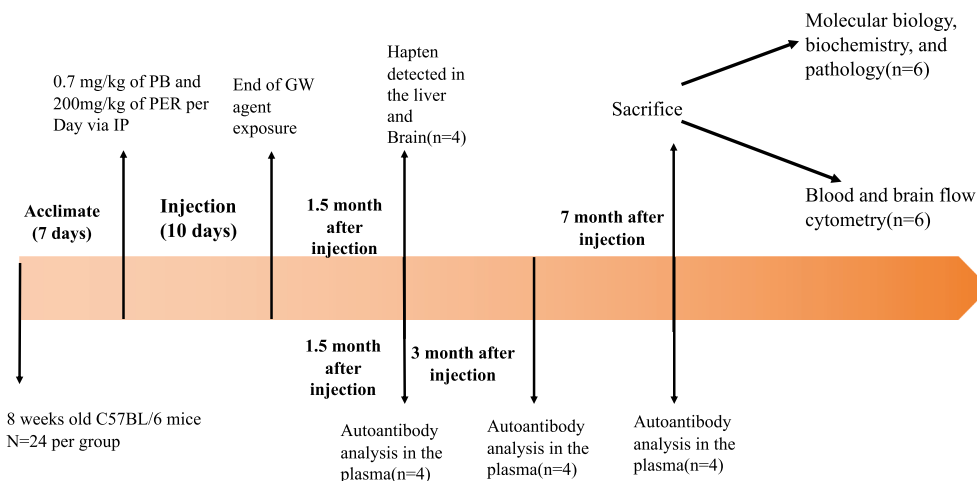
Fig. 1. Timeline of study design.

1 mL 6 M HCL at 100 °C for 2 h to hydrolyze covalent bonds between 3-PBA and proteins (Ahn et al., 2011). These samples were subjected to solid-phase extraction (SPE) using 8B-S100-UBJ Strata™-X 33 μm polymeric reversed phase, 60 mg/3mL spin columns (Phenomenex, Torrance, CA, USA) for clean-up and spiked with 10 μM phenoxy-$^{13}C_6$-3-PBA (Cambridge Isotope, Tewksbury, MA, USA) internal standard (IS). Samples were analyzed by reverse-phase liquid-chromatography/mass spectrometry (LC/MS) using a Shimadzu LC-20AT HPLC system with a 2.6 μm EVO C18 100A 100 × 2.1 mm Kinetex column (Phenomenex, Torrance, CA, USA). The mobile phases used were as follows: A (10 mM ammonium formate in water); B (100% Acetonitrile (ACN)). A gradient was run from 90% solvent A in 10% solvent B to 50% B in 6 min with a 4 min hold at 100% solvent B with a flow rate of 100 μL/min and the column temperature was set at 40 °C. Mass spectrometry analyses were conducted with high mass accuracy and parallel reaction monitoring (PRM) using a Q-Exactive (QE) hybrid quadrupole-Orbitrap mass spectrometer (Thermo Fisher Scientific, Waltham, MA, USA). Negative ion electrospray spectra were acquired at 17,500 resolution with a scan range from m/z 150 to 600. All spectra were obtained with a 100 ms maximum ion injection time and 5 microscans. The 3-PBA IS (Cambridge Isotope Laboratories, Tewksbury, MA, USA) was monitored with m/z 219.1 as the precursor mass and product ions at m/z 99.053 and 175.084. For 3-PBA, we used m/z 213.1 as the precursor ion and m/z 93.033 and 169.065 as product ions.

2.4. Quantification of 3-PBA peptide using LC/MS reverse-phase analysis

Levels of 3-PBA bound lysine in plasma, brain and liver were quantified as described by Noort et al. (2008). Briefly, 400 mg of liver and 100 mg of brain from both control and PB + PER exposed mice were homogenized in 1 mL of PBS, and protein was precipitated by the adding 4 mL of acetone at −20 °C for 3 hrs. Precipitated protein was digested with 100 μL of pronase solution (10 mg/mL, 50 mM NH4HCO3) for 1 h at 37 °C followed by analysis with LC-tandem MS as explained above. In-house synthesis of 3-PBA-albumin (described below) was as standard. The 3-PBA-lysine was monitored with m/z 343.12 as the precursor mass and product ions at m/z 197.06.

2.5. Detection of 3-phenoxybenzoic acid in urine using GC-ECD

The first urine samples of the morning were collected and frozen at −20 °C until they were analyzed for 3-PBA which was detected as described by Pakvilai et al. (2014). Briefly, 50 μL of labeled 3-PBA (1 μg/mL), as internal standard, was added to 2 mL of urine sample, then mixed for 30 s. The urine samples were subjected to acid hydrolysis by adding 500 μL of concentrated hydrochloric acid (37%) at 100 °C for 2 h. Each sample was extracted twice with 2 mL of ethyl acetate (EA), followed by centrifugation at 2500 rpm for 5 min. The organic phase was separated, and sample cleanup was then performed on pre-conditioned C18– cartridges. The resulting solution was dried and re-dissolved in acetonitrile. The 3-PBA was analyzed by using a Hewlett-Packard 7890B-electron capture detector (GC-ECD) and Autosampler G4513A (Agilent Technology, CA, USA) equipped with HP-5 (5% phenylmethyl polysiloxane with 30 m × 0.25 mm, 0.25 μm film thickness) after derivatization by 1,1,1,3,3,3-Hexafluoroisopropanol (HFIP) and N,N'-Diisopropylcarbodiim (DIC).

2.6. Preparation of 3-PBA-albumin conjugate

It has been shown that the 3-PBA metabolite of PER forms covalent adducts with albumin, and, due to its high abundance, albumin is often the major target of drug haptenation (Grigoryan et al., 2009; Tailor et al., 2016). We chose albumin to test our hypothesis that 3-PBA can also haptenate protein (3-PBA-albumin) and stimulate immune responses. We prepared a 3-PBA-albumin conjugate as described by Ahn et al. (2007). Briefly, 65 mg of 3-PBA (Sigma Aldrich, St. Louis, MO,

USA) and 92 mg 1,3-dicyclohexylcarbodiimide (DCC) (Sigma Aldrich, St. Louis, MO, USA) was dissolved in 4 mL of N,N-Dimethylformamide (DMF) (Sigma Aldrich, St. Louis, MO,USA). The active ester in 3-PBA was formed by adding 52 mg of N-hydroxysuccinimide (NHS) (Thermo Fisher Scientific, Waltham, MA USA) and allowed to react for 5 hrs at room temperature, after which 10 mL of 50 mM bovine or human serum albumin in pH 8 borate buffer was added to the solution and allowed to react overnight. The resulting precipitate containing 3-PBA-albumin was collected and dialyzed (12,000 Da) against PBS for 3 days to remove low molecular weight contaminates. For mouse studies (including blood culture studies), bovine albumin was used as previous studies have shown that mouse and bovine serum albumin (BSA) share 72% amino acid homology, and BSA is immunologically inactive in mice (Di Domizio, Dorta-Estremera and Cao, 2013). For human studies, human albumin was used.

2.7. 3-PBA-albumin autoantibody detection in the plasma

Both free albumin and 3-PBA-albumin were subjected to sodium dodecyl sulfate (SDS) polyacrylamide gel electrophoresis in 4–20% Criterion™ TGX Stain-Free™ Precast Gels (Bio-Rad, Hercules, CA, USA). These proteins were then transferred to a polyvinylidene difluoride (PVDF) membrane for 4 h at 60 mA. After blocking in 5% milk for 1 h, PB + PER mouse plasma and control mouse plasma were used as a source of antibody. The membrane was incubated in PB + PER mice or control mice plasma (1:300) overnight at 4 °C. Membranes were then incubated in HRP-linked mouse secondary anit-IgG antibody, and the blot was developed using SuperSignal West Femto Maximum Sensitivity Substrate (Thermo Fisher Scientific Waltham, MA USA) and visualized using a chemiluminescence imager (Bio-Rad, Hercules, CA, USA) as described previously (Joshi et al., 2018). For human samples, the same procedure was used with the exception that human secondary anti-IgG was used.

2.8. Ex vivo whole blood flow cytometry studies

To test our hypothesis that 3-PBA albumin can stimulate immune response and activate T- and B-lymphocytes, blood from 7-months old control mice (C57BL/6) was collected following a cardiac puncture. Blood was then combined with 2% EDTA and cultured in RPMI media (Gibco, Carlsbad, CA, USA) at 37 °C in a humidified atmosphere containing 5% CO^2 supplemented with 1% of penicillin-streptomycin solution and 10% FBS. Cultured blood was then treated with 5 μM 3-PBA-albumin, 5 μM 3-PBA and 5 μM albumin for 12 h followed by red blood cell (RBC) lysis and stained with antibodies against the cell surface markers: CD4 (Thermo Fisher Scientific, Waltham, MA, USA), CD8 (Thermo Fisher Scientific, Waltham, MA USA), CD3 (Thermo Fisher Scientific, Waltham, MA, USA), CD19 (Thermo Fisher Scientific, Waltham, MA USA), CD27 (Thermo Fisher Scientific, Waltham, MA USA) and CD45R (B220) (Thermo Fisher Scientific, Waltham, MA, USA). Detail on the antibodies used is provided in Supplementary Table S4. These cells were analyzed using Attune® NxT Acoustic Focusing Flow Cytometer (Thermo Fisher Scientific, Waltham, MA USA). Flow cytometry analyses were done using Attune® NxT software version 2.7 (Thermo Fisher Scientific, Waltham, MA, USA). Flow cytometry data were presented as total percentage change, and graphs were generated using GraphPad Prism7. CD4 + CD3 + staining was used to identify T-helper cells while CD3 + CD8 + staining was used to identify cytotoxic T-cells (Alberts and Johnson, 2002). CD19 + and CD27 + were used to distinguish memory and naïve B-cell population (Santer et al., 2013).

2.9. Detection of mouse blood monocytes and lymphocytes (B- and T-cells) using flow cytometry

Whole blood was drawn from mice, and 100 μL was subjected to red blood cell (RBC) lysis using 1 mL of RBC lysis buffer (Thermo Fisher

Scientific, Waltham, MA USA), washed twice with PBS-containing 5 mM EDTA and 0.5% FBS and stained with CD45 (Thermo Fisher, Waltham, MA USA), CD115 (BD bioscience, NJ, USA), Ly6C (BioLegend, San Diego, USA) and CD11b (BD Bioscience NJ, USA) antibodies for flow cytometry analysis. Details on the antibodies used are provided in Supplementary Table S5. Monocytes were identified by gating cells that were positive for both CD11b and CD115 (Randolph et al., 2008; Greter et al., 2015). Patrolling and infiltrating monocyte populations were identified by CD11b+ CD115+ with Ly6C- and CD11b+ CD115+ with Ly6C+, respectively (Chao et al., 2013). Ly6C+ monocytes are defined as proinflammatory and tissue-infiltrating while Ly6C++ are phagocytic monocytes (Randolph et al., 2008). Flow cytometry analysis was conducted using combinations of these monoclonal antibody using Attune® NxT Acoustic Focusing Flow Cytometer (Thermo Fisher Scientific, Waltham, MA USA).

In another experiment, 150 μL of whole blood from the same mice were lysed via addition of 1500 μL of RBC lysis buffer (Thermo Fisher Scientific, Waltham, MA, USA). The monocytes and lymphocytes were pelleted by centrifugation at $700 \times g$ for 10 min and resuspended in 500 μL of FACS buffer (PBS, 0.5–1% BSA or 5–10% FBS, 0.1%), to which 10 μL of CD4/CD8 antibody cocktail (Thermo Fisher Scientific, Waltham, MA USA) was added. Cells were incubated with the cocktail for 20 min at room temperature. Lymphocyte populations were gated, and CD4+ and CD8+ cells were analyzed using Attune® NxT Acoustic Focusing Flow Cytometer (Thermo Fisher Scientific, Waltham, MA USA). CD3+CD4+ are used to identify T-helper cells while CD3+CD8+ cells are used to identify cytotoxic T-cells. These cells were analyzed as described above. For B-lymphocytes, a combination of CD27, CD19 and CD45R (B220) stains were used as described previously; detail on antibodies used is provided above. As described previously, these were used to distinguish memory and naïve B-cell population (Santer et al., 2013).

2.10. Labeling of human PBMC for T- and B-lymphocytes

The peripheral mononuclear cells provided by GWIC (Boston) were treated with monoclonal antibodies conjugated to different fluorophores. To find the T-cell population, cells were incubated with Anti-human CD3/CD4/CD8 Cocktail (Biolegend, San Diego, CA USA). To find the memory B-cell population, a combination of CD19 (Thermo Fisher Scientific, Waltham, MA, USA) and CD27 (Thermo Fisher Scientific, Waltham, MA, USA) antibodies were used and analyzed using Attune® NxT Flow Cytometer as described above.

2.11. Flow cytometry studies of the brain myeloid and microglia cells

A single cell suspension was generated from adult mouse brains, using the adult brain dissociation kit from Miltenyi Biotec (Cologne, Germany) and closely following the manufacturer instructions. Briefly, mouse brains were collected in serum-free media and chopped finely with a sterile scalpel blade. The brains were subjected to a combination of enzymatic Papain (1 μg/μL) mechanical digestion (pipetting up and down 20 times) to yield a single cell suspension, the brain homogenate was then passed through a 70 μm strainer, and the cell suspension was centrifuged for 10 min at $1000 \times g$ and 4 °C. Cell pellets were then resuspended in debris removal solution and carefully overlaid with 4 mL D-PBS as per manufacturer instructions; the samples were then centrifuged at $3000 \times g$ for 10 min at 4 °C in a swinging bucket rotor with minimal brake. Following centrifugation, four phases were formed in the tube, the upper 2 phases were aspirated, the remaining (glia cell containing) fraction was then resuspended in PBS, inverted multiple times and centrifuged at $1000 \times g$ for 10 min to generate a pellet containing a mixed glial cell population. The myeloid populations were then isolated by magnetically activated cell sorting (MACS), using anti-CD11b conjugated magnetic microbeads (Miltenyi Biotec, Cologne, Germany) according to the manufacturer's protocol. Briefly, cells were

incubated with 10 μL CD11b coated microbeads for 15 min at 4 °C. Cells were then washed and placed on a new LS magnetic column (Miltenyi Biotec, Cologne, Germany) in a magnetic holder. The CD11b negative fraction was washed through the column, and the CD11b positive cell fraction was eluted from the column by removing the column from the magnetic field, adding buffer and emptying the column with a plunger. Cells were incubated with Rat anti-mouse Fc-block (1:100 BD bioscience) for 5 min at room temperature. These cells were then stained with monoclonal antibodies for desired surface markers. The antibodies used were CD11b (BioLegend San Diego, USA), CX3CR1 (BioLegend, San Diego, USA), Ly6c (BioLegend San Diego, USA) and CD206 (BioLegend San Diego, USA). Details on the antibodies used are provided in the Supplementary Table S6. These cells were analyzed as described above using an Attune® NxT Acoustic Focusing Flow Cytometer (Thermo Fisher Scientific, Waltham, MA USA). A combination of CD11b+, CX3CR1+, CD206+, and Ly6C+ staining was used to analyze brain macrophages, and cells stained with CD11b+, CX3CR1+, and CD206− were classified as microglia (Han et al., 2015; Wong et al., 2017; Zhou et al., 2017; Zarruk et al., 2018).

2.12. Immunostaining for microglia and astrocytes

The left-brain hemispheres were fixed in 4% paraformaldehyde (PFA), dehydrated and embedded in paraffin. Sagittal sections (8 μm) were prepared using Leica RM2235 microtome (Leica, Buffalo grove, IL). Approximately 8 to 10 slices of each mouse brain were incubated in blocking buffer (10% donkey serum and 0.3% Triton X-100 in PBS) for 60 min at room temperature. Samples were then incubated overnight with the primary antibody Rabbit anti-IBA-1 (Wako, Osaka, Japan) and Chicken anti-GFAP (Aves Lab, Tigard, Oregon) at 4 °C. The following day, slices were incubated with the appropriate fluorescent probe-conjugated secondary antibodies for 1 hr at room temperature. Nuclei were counterstained with DAPI. The entire DG was scanned using an Axiovert 200 M Zeiss microscope (Zeiss) equipped with AxioVision 4.8.3.0 software. ImageJ software was used to analyze the stained sagittal sections. The stained areas were calculated and expressed as a percentage of the field. Further detail on primary and secondary antibodies used for brain pathology is provided in Supplementary Table S7.

2.13. Enzyme-linked immunosorbent assay

Using a Dounce homogenizer, brains were homogenized in ice cold Mammalian Protein Extraction (mPER) buffer (Thermo Fisher Scientific, Waltham, MA USA), which contained protease (Roche, Indianapolis, IN, USA) and phosphatase inhibitor (Pierce, Grand Island, NY, USA) cocktails. These whole brain homogenates were centrifuge at $10,000 \times g$ for 10 min, and supernatant was used for ELISA and Western blot. The total protein content of each sample was determined by the bicinchoninic acid (BCA) assay (Pierce, Grand Island, NY, USA). Enzyme-Linked Immunosorbent Assay (ELISA) kits for mouse CCR2 (Lifspan Biosciences, Seattle, WA,USA), CCL2 (Lifspan Biosciences, Seattle, WA, USA), Matrix Metalloproteinase-9 (MMP9) (Bosterbio, Pleasanton, CA, USA) and fractalkine (CX3CL1) protein (MyBiosource, San Diego, CA,USA) were used to study levels of these proteins in the brain using the manufacturer's protocol. Soluble CX3CL1 (Thermo Fisher Scientific, Waltham, MA USA) in human plasma were quantified using a commercial ELISA kit. The level of IgG protein in blood was quantified by IgG ELISA (Cayman Chemical, Ann Arbor, MI, USA) according to the manufacturer's instruction. MMP9 is a proteolytic protein capable of degrading tight junction protein leading to BBB impairment (Underly et al., 2016; Schactae et al., 2017). Results were normalized to total protein quantification obtained from BCA. Intra-Assay: CV < 10.6% Inter-Assay: CV < 12.6% for all the ELISAs. There was no reported cross-reactivity with other proteins for the primary antibody used in these kits.
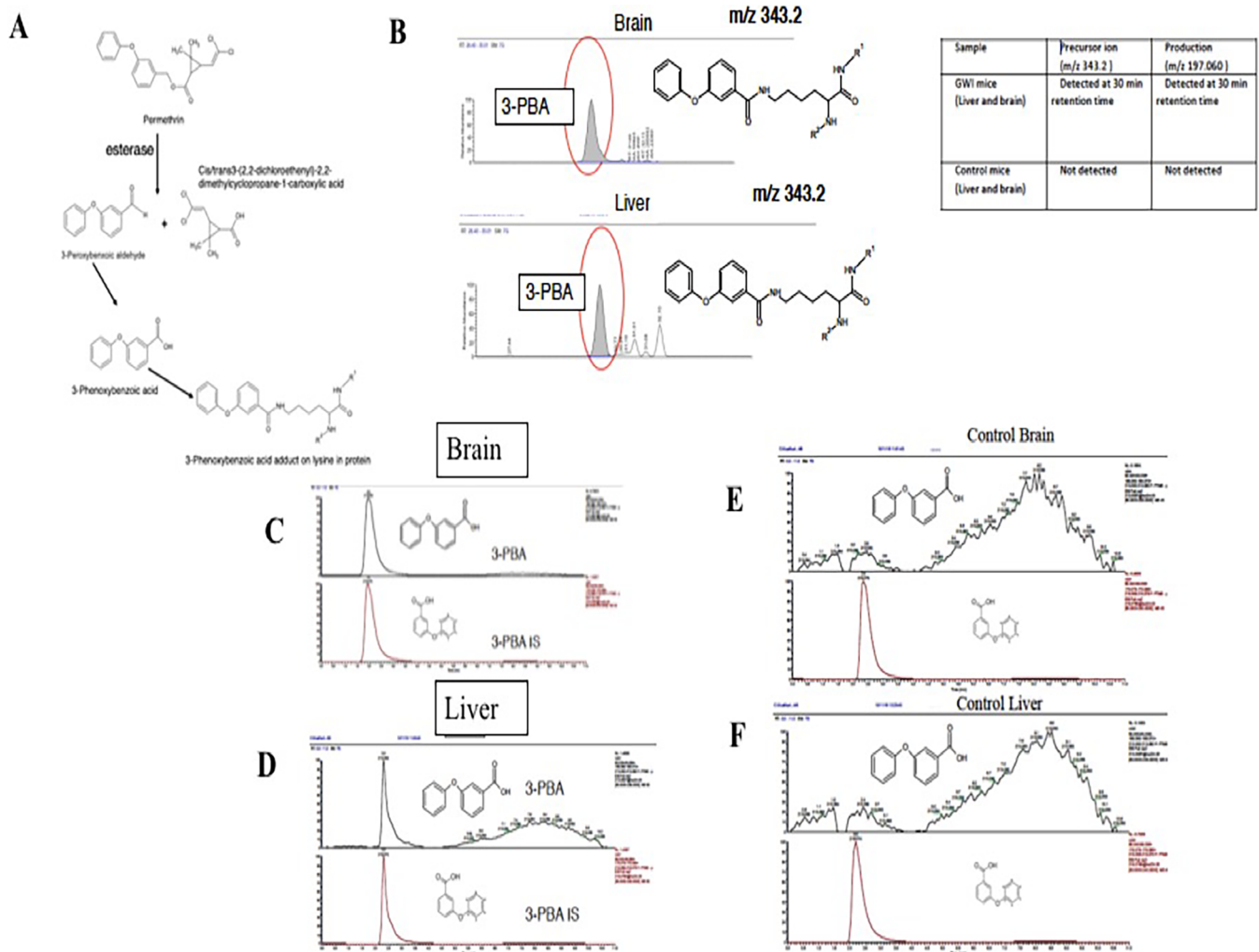
Fig. 2. Metabolites of PER pesticide is detected as protein adducts in the brain and liver homogenates. (A) A schematic of PER metabolites. (B) Detection of precursor and product ion of 3-PBA lysine (343.2) and its product ions (197.06) in the brain and liver homogenates from a GWI mouse sample. (C and D) Using LC-MS and LC-MS/MS, we detected 3-PBA (m/z 213.055 at 3 min) and its PRM product ion (m/z 213.1 > 93.033 at that same time) in the brain and liver (mean ± SE (n = 4 or 5/group). While only protein-conjugated 3-PBA recovered after hydrolysis was detected in the brain, free 3-PBA and protein-conjugated 3-PBA were detected in the liver at 1.5 months post-exposure. (E and F) Peak plots show absence of 3-PBA (m/z 213.055 at 3 min) and its transition ion (m/z 93.033) ions in control mice. These peak plots show presence of 3-PBA internal standard 219.1 at 3 min and its transition ion (m/z 93.033) ions in control mice.

2.14. Western blot analyses

CX3CR1 (Abcam, Cambridge, MA, USA), p-65(p-NFκB) phosphory-lated at Ser536 (Cell Signaling, Danvers, MA, USA), total p65 (NFκB) (Cell Signaling, Danvers, MA, USA), tubulin (Abcam, Cambridge, MA, USA), major histocompatibility complex-II (MHC-II) (Abcam Cambridge, MA, USA), actin (Cell signaling, Danvers, MA, USA) and occludin (Santa Cruz biotechnology, Santa Cruz, CA, USA) were ana-lyzed using Western Blotting. MHC-II are markers of antigen-presenting cells (Lehnardt et al., 2003; Vaure and Liu, 2014). In the brain, mi-croglia and macrophages are the main cells expressing MHC-II (Lehnardt et al., 2003). Occludin is a tight junction protein used to analyzed BBB impairment (Liebner et al., 2000; Yang et al., 2017). Western Blotting was performed as described previously (Joshi et al., 2018). A list of primary antibodies used is provided in the Supplementary Table S8 along with the dilutions and sources. Horse-radish peroxidase-conjugated appropriate secondary antibodies and loading control anti–β-actin or tubulin antibody was obtained from Cell Signaling. The blots were analyzed as described previously (Joshi et al., 2018). Briefly after the BCA (as described above), 20 μg of protein from whole brain homogenate were heated with Laemmli buffer containing beta-mercaptoethanol (BioRad, Hercules, CA, USA) and separated by gel electrophoresis using 4–15% Criterion™ TGX Stain-Free™ Protein Gel, (Biorad, Hercules, CA, #5678085) and then transferred to a PVDF membrane (Biorad, Hercules, CA) overnight at 90 mA. The membranes were blocked for 1 h in 5% blocking milk (BioRad, Hercules, CA, USA). Then, each membrane was individually immunoprobed with a primary antibody in blocking buffer overnight. After each primary antibody incubation, each membrane was incubated with the recommended di-lution (1:5000) of corresponding horseradish peroxidase-conjugated secondary antibody (cell signaling) in blocking buffer at room tem-perature for one hour. Protein bands were visualized using enhanced chemiluminescence detection reagents (Thermo Scientific, MA USA). Band intensities were analyzed using the ChemiDoc imaging system (Bio-Rad). Results were calculated using Image Lab software and nor-malized to the expression of actin protein in the samples.

2.15. Multiplex cytokine assay

Selected cytokine levels in the plasma were analyzed using Meso Scale Discovery (MSD) 96-Well MULTI-SPOT® Ultra-Sensitive V-PLEX Proinflammatory cytokine Panel 1 mouse Kit (MSD, Rockville, MD,

USA), using electrochemiluminescence detection on an MSD Sector Imager™ 6000 with Discovery Workbench software (version 3.0.18) (MSD®, Gaithersburg, MD, USA). Cytokines were measured using the TH1/TH2 8-plex kit which included interleukin-1β (IL-1β), IL-6, interferon-γ (IFN-γ) and tumor necrosis factor-α (TNFα). All assays were performed according to the manufacturer's instructions, in duplicates as described previously (Joshi et al., 2018). Human plasma was analyzed using V-PLEX Proinflammatory cytokine Panel 1 Human Kit (MSD, Rockville, MD, USA) according to manufacturer protocol.

2.16. Statistical analyses

Normally distributed data were analyzed using parametric tests; otherwise non-parametric tests were used. As applicable, the Student's *t*-test was used to examine the group differences between PB + PER mice and control mice for cytokines, chemokines, percentage of specific cells identified using flow cytometry and protein levels of p-NFκB, occludin, MMP9, IgG and MHC-II. Murine cytokine data were analyzed by using the Student's *t*-test. Human cytokine data were not normally distributed, so the Kolmogorov-Smirnov test (K-S test) was performed on them to check if they were statistically significant. For autoantibody analysis in the GW veteran cohort, the Chi-square test was performed to determine statistical significance. For multiple groups in blood culture studies, we used one-way analysis of variance (ANOVA) followed by the Tukey *post-hoc* test. A *p* value < 0.05 was considered statistically significant. These analyses were performed using GraphPad Prism7 (San Diego, CA, USA), and data were expressed as means $\pm$ standard errors. All graphs were generated using GraphPad Prism7 (San Diego, CA, USA).

3. Results

3.1. Detection of 3-PBA released following protein hydrolysis and 3-PBA-modified lysine residues from peptides in the brain, liver and plasma of PB + PER mice

For an acute post-exposure timepoint, we examined 3-PBA modified proteins in liver, brain and plasma of PB + PER exposed mice euthanized at 1-day post-exposure. We also examined a serum sample of a subject positive for 3-PBA in urine as a positive control. Fig. 2 shows PER metabolite structures and detected ions that correspond with the presence of 3-PBA lysine residues after pronase digestion that was performed to release these adducts from peptides (Fig. 2B). We also quantified 3-PBA released post-protein-hydrolysis which showed the presence of 3-PBA in the livers and brains of PB + PER mice at 1.5 months post-exposure (Fig. 2C and 2D). However, free 3-PBA was detected only in the livers but not in the brains of exposed mice. As expected, no 3-PBA was detected in control mice (Fig. 2E and 2F). Neither free nor protein-conjugated 3-PBA was detected in the brains or livers of exposed mice at 3- or 7-months post-exposure.

3.2. 3-PBA-albumin autoantibodies in plasma from PB + PER mice and in GWI veterans.

Western blot analyses showed that while plasma from control mice did not have immunoreactivity to free albumin or 3-PBA-albumin, plasma from PB + PER exposed mice showed a strong immunoreactivity with 3-PBA-albumin but not with free albumin (Fig. 3A). We then examined if 3-PBA human albumin-reactive autoantibodies were detectable in plasma from GW veterans. Plasma from 10 out of 12 GW veterans diagnosed with GWI showed immunoreactivity to 3-PBA-albumin, and 1 out of 10 healthy GW veterans had immunoreactivity to 3-PBA albumin ($\chi^2 = 11.73$, df = 1, $p = 0.001$, Fig. 3B). Details of these antibodies detected is provided in table 1A. None of the plasma samples from GW veterans showed any immunoreactivity to albumin alone (Fig. 3B). There was a significant

association between self-report of pesticide exposure and 3-PBA-albumin autoantibody presence among veterans with GWI ($\chi^2 = 9.46$, df = 1, $p = 0.03$). Only one control GW veteran had 3-PBA-albumin autoantibodies and was exposed to pesticides. Additionally, this control GW veteran reported being exposed to PER but not to PB and autoantibodies against 3-PBA-albumin were still detected in plasma. Also, no 3-PBA-albumin autoantibodies were detected in plasma from one GWI case who was exposed to PB but not PER. Two additional controls who didn't have autoantibodies did report pesticide exposure, where one subject had an exposure to fogged area whereas the other subject did report exposure to pesticide imbedded uniforms, creams and sprays. In another cohort from Thailand, we detected 3-PBA-albumin autoantibodies in the serum of 5 subjects who had positive 3-PBA urine levels, whereas 5 control serum samples with undetectable urinary 3-PBA levels did not show immunoreactivity to 3-PBA-albumin (Fig. 3C). Both human and mice secondary antibody alone showed no cross reactivity with albumin or 3-PBA-hapten (Supplementary Fig. S7).

3.3. Peripheral T-cells and B-cells activated following 3-PBA-albumin treatment

Murine blood was cultured overnight to examine if 3-PBA-albumin as compared to albumin alone, 3-PBA alone and control treatments can activate B-cells, T-cells and monocytes. Antigen-responsive CD19 + CD27 + B-cells were significantly different between the four groups ($F_{(3,12)} = 12.2$, $p = 0.001$, Fig. 4A), with the 3-PBA-albumin group being significantly elevated compared to all other groups (*post-hoc* $p < 0.05$). Consistently, IgG levels were increased by 3-PBA-albumin treatment compared to all other groups ($F_{(3,12)} = 221.8$, $p = 0.001$ Supplementary Fig. S1A). Group comparisons for CD3 + CD4 + T-helper cells showed significant differences between treatments ($F_{(3,16)} = 61.19$, $p = 0.001$, Fig. 4B) with *post-hoc* analyses showing increases in CD3 + CD4 + T-helper cells by 3-PBA-albumin treatment as compared to controls, 3-PBA and albumin alone ($p < 0.05$). There were no differences in CD3 + CD8 + T-lymphocytes when treated with 3-PBA-albumin compared to all other treatments ($p > 0.05$). Total monocyte population gated by CD11b + and CD115 + differed significantly between the groups ($F_{(3,12)} = 20.48$, $p = 0.001$, Supplementary Fig. S1B), and *post-hoc* comparisons showed an increase in these cells in the 3-PBA-albumin group compared to others ($p < 0.05$).

3.4. Activated peripheral immune cells and plasma proinflammatory cytokines are increased in the blood of PB + PER mice and veterans with GWI

An antigen-reactive B-cell population positive for CD45 + CD19 + CD27 + was elevated in the blood of PB + PER mice compared to control mice (*t*-test$_{(df=6)} = 5.7$, $p = 0.0012$, Fig. 5A). However, the CD19 + CD27 − population did not differ between the two groups ($p > 0.05$), suggesting that while total B-cell population doesn't change, antigen-responsive B-cells proportionally increase. Higher levels of IgG were present in blood from PB + PER exposed compared to control mice (*t*-test$_{(df=5)} = 4.5$, $p = 0.008$, Supplementary Fig. 1C). We analyzed CD4 + and CD8 + markers after gating on the blood lymphocyte population. This study revealed that CD4 + T-helper cell population was significantly higher in the lymphocytes of exposed compared to control mice (*t*-test$_{(df=7)} = 2.7$, $p = 0.024$, Fig. 5B). T-helper cells expressing CD3 + CD4 + were also elevated in the blood of PB + PER exposed mice (*t*-test$_{(df=6)} = 5.3$, $p = 0.0017$, Fig. 5B). Although CD8 + lymphocytes didn't differ between the two groups ($p > 0.05$), the ratios of CD4 + to CD8 + cells were elevated in PB + PER exposed compared to control mice (*t*-test$_{(df=6)} = 3.7$, $p = 0.0014$, Fig. 5B). Mouse monocytes defined by CD11b + and CD115 + cells were elevated in PB + PER exposed compared to control mice (*t*-test$_{(df=11)} = 4.2$, $p = 0.0012$, Supplementary Fig. S2). In
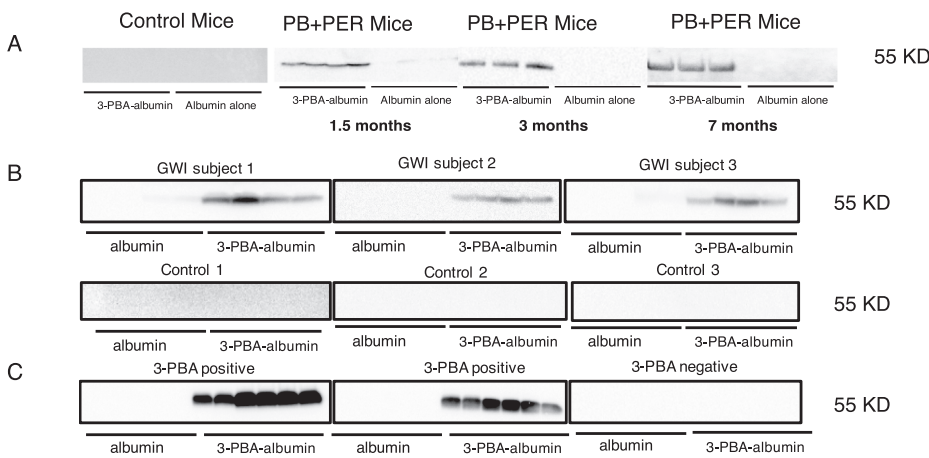
Fig. 3. Chronic elevation of autoantibodies against 3-PBA-albumin in plasma of PB + PER mice, in veterans with GWI and in farm workers exposed to pyrethroids. Western Blot showed that control mice had no cross-reactivity to 3-PBA-albumin or albumin alone, but cross-reactivity in PB + PER mice plasma was observed for 3-PBA-albumin at 1.5-, 3- and 7-months post-exposure in PB + PER mice (n = 4 or 5/group). (B) Autoantibodies against 3-PBA-albumin were detected in 12 out of 14 veterans with GWI and 1 out of 10 control GW veterans. (C) Immunoreactivity of plasma with 3-PBA-albumin was observed in 5 out of 5 pyrethroid-exposed farm workers or ate pyrethroid tainted fruits and vegetables (as confirmed using 3-PBA measurements in urine), and a lack of immunoreactivity in controls in whom urine 3-PBA was undetected.

addition, at 7 months post-exposure, several proinflammatory cytokines, including IL-1β, IL-6, IFN-γ and TNF-α and a chemokine CX3CL1 were elevated in the brain and plasma from this PB + PER mouse model (Supplementary Fig. S3).

We also examined peripheral T- and B-cells in PBMCs from GWI and control GW veterans. The memory B-cell population, as defined by CD19 + CD27 + cells, was significantly increased in GWI compared to healthy GW veterans (t-test$_{(df=20)}$ = 5.01, p = 0.0014, Fig. 6A). T-helper cells expressing CD3 + CD4 + are also elevated in GWI veterans (t-test$_{(df=28)}$ = 8, p = 0.001, Fig. 6B). Although CD3 + CD8 + T-cells didn't differ between the two groups (p > 0.05), the ratios of CD4 + to CD8 + cells were elevated in GWI compared to control GW veterans (t-test$_{(df=20)}$ = 3.7, p = 0.0014). Compared to healthy GW veterans, plasma levels of proinflammatory cytokine IL-1β and CX3CL1 were higher in veterans with GWI (Supplementary Fig. S4).

### 3.5. Disruption of the BBB in PB + PER mice

Since MMP9 is increased during inflammation, we examined MMP9 levels in the brain homogenates from PB + PER mice and control mice. MMP9 was significantly higher in the brains of PB + PER exposed mice (t-test$_{(df=9)}$ = 2.7, p = 0.028, Fig. 7B). Assessment of BBB integrity examined using occludin showed a significant decrease in PB + PER exposed mice compared to control mice (t-test$_{(df=10)}$ = 2.5, p = 0.029, Fig. 7A). Increases in brain IgG levels are generally indicative of BBB impairment, and levels of IgG were increased in the brains of PB + PER exposed mice compared to controls (t-test$_{(df=9)}$ = 3.71, p = 0.043, Fig. 7B).
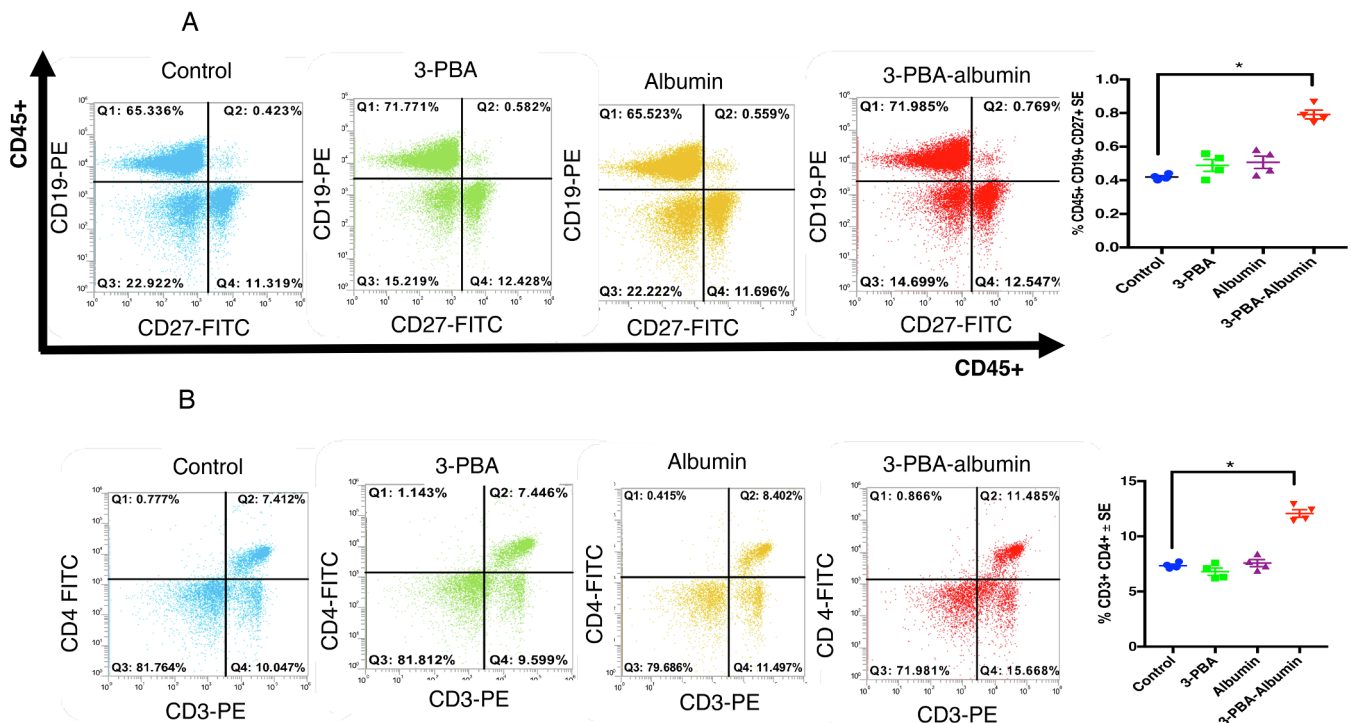
Fig. 4. 3-PBA-albumin treatment increased memory B-cell and T-helper cells in 7 months old control mice. Mean ± SE (n = 4 per group). (A) After overnight incubation of murine blood with 3-PBA, albumin and 3-PBA-albumin, antigen-responsive CD45 + CD19 + CD27 + B-cells are significantly elevated in 3-PBA-albumin compared to all other treatments. (B) T-helper cells, CD3 + CD4 +, were also elevated upon 3-PBA-albumin treatment. Comparisons between 3-PBA and controls and albumin and controls were not significant. *p < 0.05.
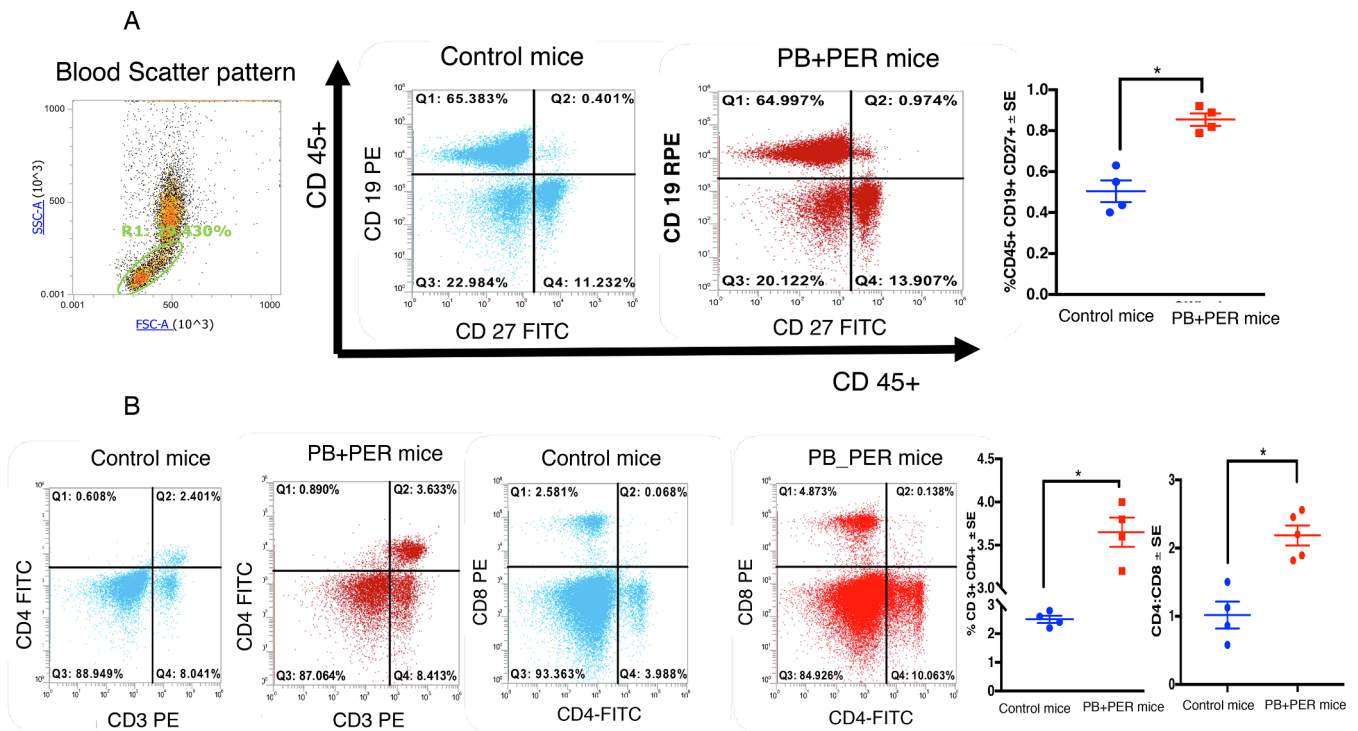
Fig. 5. Antigen-activated B- and T-cells are increased in blood of PB + PER mice at 7 months post-exposure. Mean ± SE (n = 4/5 per group). (A) Increased staining of antigen-responsive CD19+ CD27+ B-cells were detected in GWI compared to control mice. (B) Panel B shows that CD3+CD4+ T-cells are increased in blood of PB + PER mice. However, CD8+ T-cells did not differ between the two groups. Ratios of CD4:CD8 was significantly elevated in PB + PER mice. *p < 0.05.
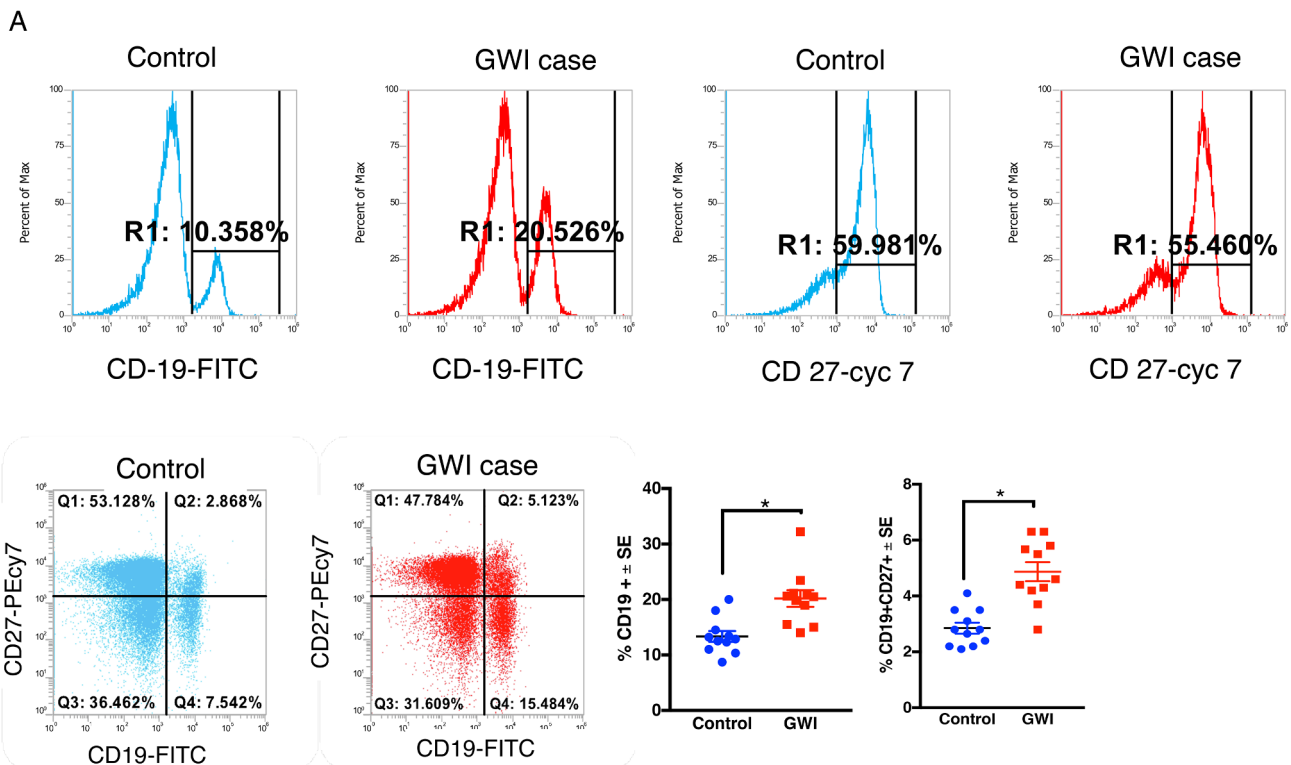
Fig. 6. Memory B- and CD4 T-cells are increased in blood of veterans with GWI. Mean ± SE (n = 12 per group). (A) Increased staining CD19+ and CD19+ CD27+ memory B-cells in blood of veterans with GWI compared to healthy GW control veterans. (B) CD3+ CD4+ T$_H$ cells are increased in blood of veterans with GWI. However, CD8+ T$_H$ cells did not significantly differ between control and GWI veterans. However, there were no group differences for CD3+CD8+ T$_H$ cells. *p < 0.05.
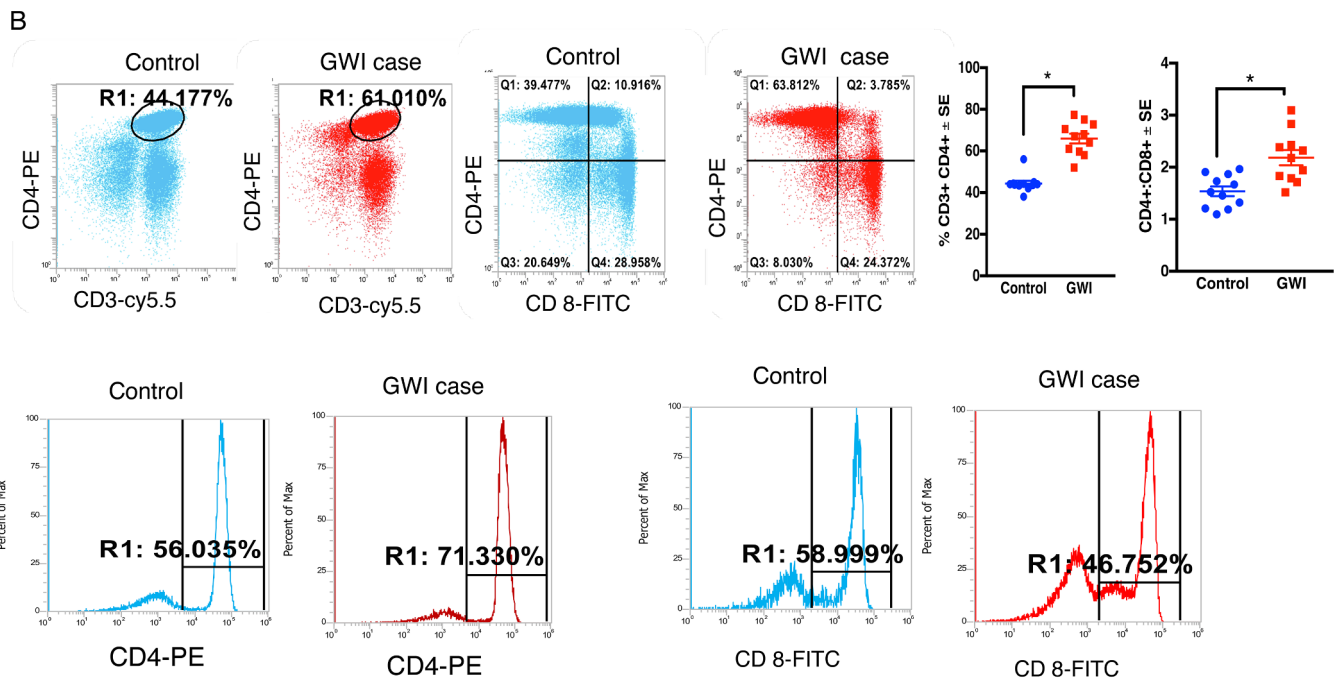
B

Fig. 6. (*continued*)

3.6. Infiltrating monocyte population in the blood and brain of PB + PER mice

Monocytes staining with CD11b+ CD115+ and Ly6C+ classified as proinflammatory and infiltrating were elevated in PB + PER exposed mice blood compared to control mice (t-test$_{(df=11)}$ = 3.7, p = 0.0032, Fig. 8A). Macrophages were detected using CD11b+ CD206+ Ly6C+ positive stains, which were increased in the brains of PB + PER exposed mice compared to control mice (t-test$_{(df=2.8)}$ = 4.7, p = 0.04, Fig. 8B). The microglia population characterized by CD11b+, CX3CR1+, CD206− Ly6C− showed no differences between the two groups (Fig. 8C). Infiltrating monocytes detected by CD11b+ CX3CR1− Ly6C+ were significantly increased in the brains of exposed mice compared to controls (t-test$_{(df=4)}$ = 4.7, p = 0.01, Fig. 8D). Patrolling monocyte populations (CD11b+ CX3CR1+) were significantly increased in the brain of PB + PER exposed mice (t-test$_{(df=6)}$ = 6.2,

p = 0.032, Supplementary Fig. 2B). We also observed increased MHC-II protein levels in the brains of PB + PER exposed mice compared to controls (t-test$_{(df=6)}$ = 6.2, p = 0.0007, Fig. 8E).

3.7. Chemokines and their receptors that promote CNS and peripheral immune cross-talk are increased in PB + PER mice

Since plasma CX3CL1 levels were increased in PB + PER exposed mice and in veterans with GWI (Supplementary Figs. 3 and 4), we examined its receptor CX3CR1 in the brain homogenates from PB + PER mice and control mice at 7-months post-exposure. Levels of CX3CR1 were elevated in PB + PER mice compared to control mice (t-test$_{(df=5)}$ = 3.1, p = 0.03, Fig. 9A). There were no differences in the membrane fraction of the brain homogenates for CX3CL1 levels between PB + PER exposed mice and control mice at 7-months post-exposure (p = 0.86, Fig. 9B). Levels of CCR2 (t-test$_{(df=10)}$ = 4.71,
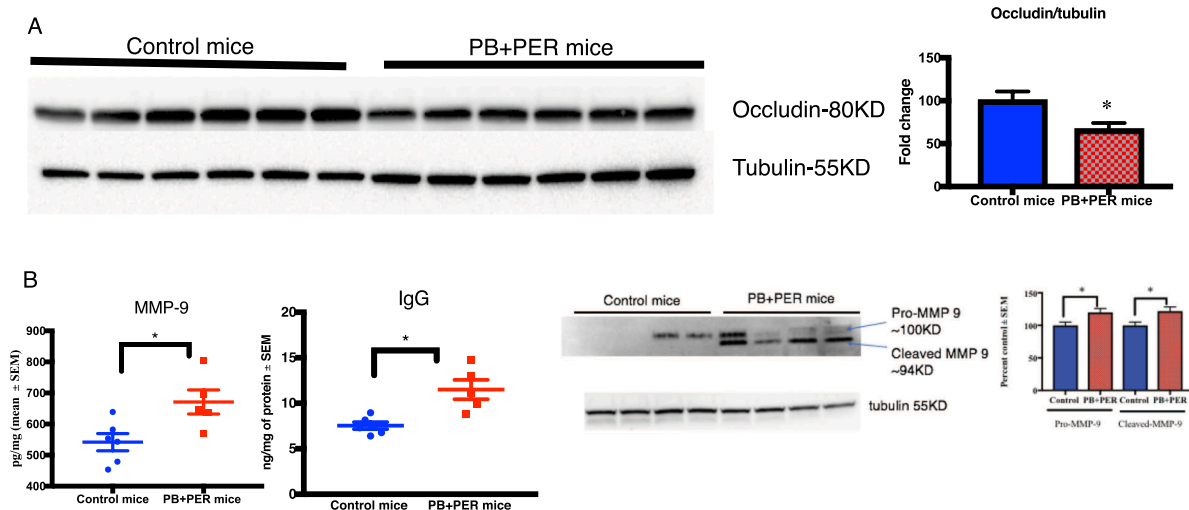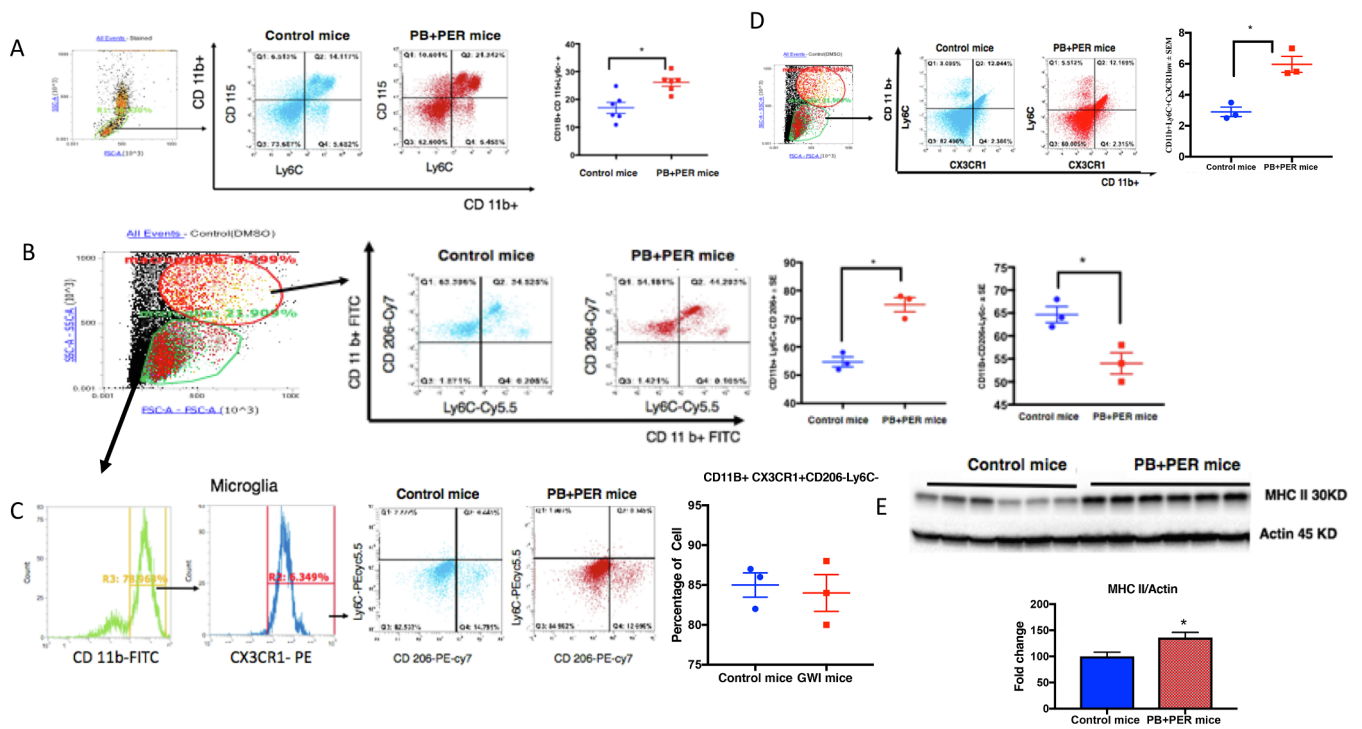
A

B

Fig. 7. PB + PER mice showed evidence of BBB impairment. Mean ± SE (n = 6 per group). (A) Occludin was decreased in the brains of PB + PER mice whereas (B) MMP-9 and IgG were increased in PB + PER mice brain. (C) Representative images of MMP-9 western blot of whole brain homogenate. Band intensities from control and PB + PER animal brain tissue (n = 4). *p < 0.05.

Fig. 8. Infiltrating monocytes are increased in blood and brains of PB + PER mice at 7–8 months post-exposure. Mean ± SE (n = 12 per group) (A) Increases in blood monocyte gated by CD11B+ CD115+ and Ly6C+ in PB + PER mice were observed. (B) PB + PER mice brain showed increased macrophage population as detected by CD11b+CD 206+Ly6C+ but (C) no change in microglia population detected by CD11b+CX3CR1+ and CD206−. (D) Infiltrating monocytes converting to macrophage (CD11b+, CX3CR1− and Ly6C+) were also increased in the brains of PB + PER mice. (E) Increase in MHC-II in the brain of PB + PER mice was detected by Western Blot *$p < 0.05$.
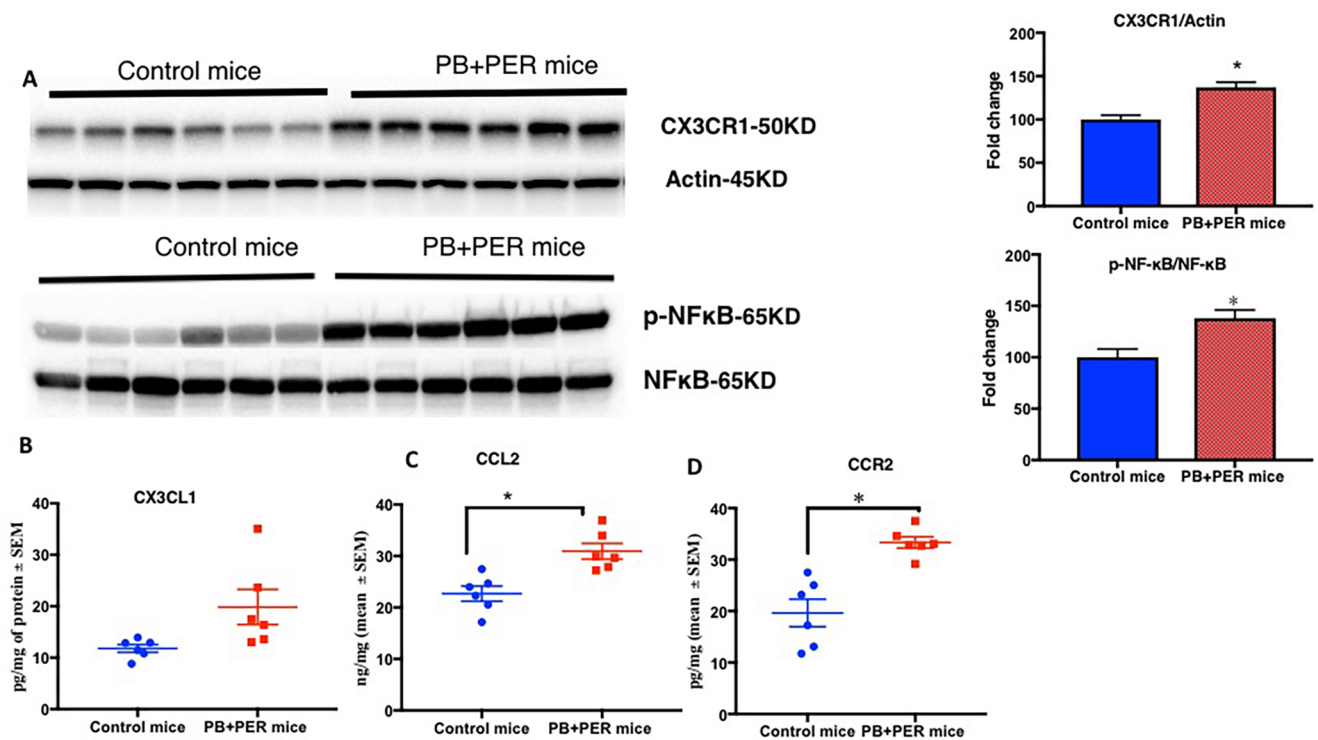
Fig. 9. CCR2 and its ligand CCL2 are chronically increased in the brains of PB + PER-exposed mice leading to inflammation. Mean as % control ± SEM (n = 6 per group). (A) Western Blot showing CX3CR1/actin and pNFκB/NFκB is increased in the brains of PB + PER-exposed mice. (B) No change in CX3CL1 level as measured by ELISA. (C) Levels of CCL2 were also increased in PB + PER-exposed mice at 7-months post-exposure. (D) CCR2 levels were increased in the brains of PB + PER mice. *$p < 0.05$.

$p = 0.0008$, Fig. 9C) and its ligand CCL2 (t-test$_{(df=10)}$ = 3.9, $p = 0.003$, Fig. 9D) were increased in the brains of PB + PER exposed mice compared to control mice. Immunohistochemistry work showed astroglia activation in the dentate gyrus and cortex of PB + PER mice compared to control mice (Supplementary Fig. S5). We examined the ratios of phosphorylated p65 (p-NFκB) to total p65 (NFκB) in PB + PER exposed mice to assess inflammation. There was a significant increase in p-NFκB/NFκB ratios (t-test$_{(df=5)}$ = 2.2, $p = 0.06$, Fig. 8A). *Post-hoc* analyses showed that the ratios of p-NFκB/NFκB were increased in PB + PER mice at this 7-months post-exposure timepoint.

4. Discussion

Evidence suggests that overexposure to PB and pesticides, which included pyrethroids and organophosphates, was one of the etiological factors in GWI (Binns et al., 2008; White et al., 2016; Sullivan et al., 2018). Exposure to these compounds has been shown to induce chronic immune dysfunction (Broderick et al., 2013; Craddock et al., 2015; Jokanović, 2018). While clinical symptoms of GWI resemble those of autoimmune diseases, the exact mechanism by which GW chemicals caused immune activation remains unknown. In this translational study, we show that a common pyrethroid metabolite, 3-PBA, can haptenate albumin, which activates CD4+ T-helper and antigen-responsive B-cells. These immune cells were elevated in PB + PER exposed mice and in veterans with GWI. We observed autoantibodies against 3-PBA-albumin in our PB + PER mouse model and in veterans with GWI at chronic post-exposure timepoints. In this PB + PER mouse model, we also show that brain macrophages thought to be derived from peripheral blood monocytes were increased in the brains of PB + PER exposed mice. These studies suggest that activation of autoimmune responses against endogenous proteins modified by 3-PBA corresponds with activation of brain macrophages and neuroinflammation in PB + PER exposed mice. The work described herein could aid in the development of sensitive and specific biomarkers for diagnosing GWI in order to provide appropriate care and treatment to veterans with GWI.

During the 1991 GW, a large proportion of veterans were using pyrethroid-based pesticides routinely (Binns et al., 2008; Sullivan et al., 2018). To date, accurate diagnosis of GWI remains an unmet need for ill GW veterans. One reason it is difficult to accurately diagnose GWI is because the diagnosis is based on self-report of symptoms and exposures. Since studies have shown that 3-PBA can form adducts with lysine residues on endogenous proteins (Noort, Benschop and Black, 2002; Noort et al., 2008; Thiphom et al., 2012), we performed this experiment and found a presence of 3-PBA-lysine residues in the brain, blood and liver of PB + PER exposed mice acutely after GW chemical exposure. We also examined 3-PBA recovered after protein hydrolysis and found it to be present at 1.5 months after exposure to PB and PER but not at later post-exposure timepoints. This suggests that 3-PBA-haptenated proteins are eventually eliminated. Small molecules which haptenate endogenous proteins can elicit adaptive immune responses, ultimately resulting in B-cell activation and autoantibody production (Naisbitt et al., 2002; Palm and Medzhitov, 2009). Since albumin is easily haptenated by drugs due to its abundance in blood and availability of lysine residues that can be covalently modified (Tailor et al., 2016), albumin was chosen for haptenation studies with 3-PBA. Our observations of autoantibodies against 3-PBA-albumin in blood from PB + PER exposed mice, veterans with GWI and pyrethroid-exposed subjects suggest that 3-PBA-albumin is capable of provoking autoimmune responses. These studies for the first time provide evidence of autoantibodies following pyrethroid exposure in veterans with GWI. The specificity of these autoantibodies to pyrethroid exposure is further supported by the observation of 3-PBA-albumin autoantibodies in subjects with detectable urinary 3-PBA levels and observable 3-PBA-lysine adducts in their serum. While it remains to be determined if autoantibodies against 3-PBA-albumin have a pathological role in GWI,

a higher prevalence of these autoantibodies in GWI veterans compared to control GW veterans suggests that they could be useful biomarkers of GWI.

Our animal and human studies suggest that autoantibodies against 3-PBA-albumin persist for a long time, despite the fact that 3-PBA is not detected in the brain or the liver beyond 1.5 months post-exposure. Studies have shown that proteins haptenated by other chemicals can directly interact with APC, which then travel to the lymphatic system where they present these antigens to T- and B-cells (Karlsson et al., 2018). This may result in the production of autoantibodies against haptenated proteins (Lanzavecchia, 1985; Gefen et al., 2015; Karlsson et al., 2018). While the exact mechanism behind the persistence of autoantibodies against 3-PBA-albumin remains to be investigated, it may involve a similar mechanism which requires memory B-cell activation and subsequent autoantibody production by plasma B-cells (Ochsenbein et al., 2000; Alberts and Johnson, 2002). As mentioned above, we show that autoantibodies against 3-PBA-albumin are generated in our PB + PER mouse model. Furthermore, results of our *in vitro* blood culture studies suggest that the adaptive immune system is engaged in promoting immune cell activation after 3-PBA-albumin treatment, which is characterized by an elevation of antigen-presenting monocytes, CD3+CD4+ T-helper cells and antigen-responsive CD19+ CD27+ B-cells. Interestingly, these cells did not react to 3-PBA or albumin alone, further strengthening the concept that chemical haptenation of albumin is required to elicit adaptive immune responses and that 3-PBA alone cannot promote immune activation. Increases of CD3+CD4+ T-helper and CD19+ CD27+ B-cells, together with the presence of autoantibodies against 3-PBA-albumin in PB + PER mice and in GWI veterans, further support an autoimmune-type response in GWI. These studies provide support for an activation of the adaptive immune system in GWI and are consistent with those conducted by Vojdani and Thrasher (2004), showing an elevation of CD4+ T-helper cells and B-cells in the blood of veterans with GWI. Together, these findings suggest that 3-PBA-albumin can stimulate peripheral immune cell activation.

While most veterans deployed in the GW conflict self-report the use of PB, it is unlikely that PB alone is a major contributing factor in the overactive immune responses noted in veterans with GWI. On the contrary, previous research has suggested that PB is able to suppress inflammation in rodent models (Macht et al., 2019), with exposure to PB alone resulting in decreased production of pro-inflammatory cytokines such as IL-6, IFN-y and TNF-α at chronic time points (Macht et al., 2018). However, we, along with others, have shown that these cytokines are elevated in plasma from veterans with GWI (Broderick et al., 2011; Khaiboullina et al., 2015). The mechanism of PB is well defined in the literature, acting as a reversible acetylcholinesterase (AchE) inhibitor (Musilek et al., 2011). As such, PB use would likely result in an increase in acetylcholine (ACh) levels in the periphery (Musilek et al., 2011). Recent evidence suggests a role of ACh in stimulating anti-inflammatory responses in the periphery via a direct interaction with nicotinic receptors on peripheral immune cells (Tracey, 2005; Ibrahim et al., 2018). Therefore, one would expect a dampened immune response in PB + PER exposed mice. However, since we observe activated immune responses and the presence of 3-PBA-albumin autoantibodies in plasma of both human and PB + PER exposed mice, it is possible that PB was unable to suppress immune cell activation that occurs in the presence of combined PB + PER exposure (Joshi et al., 2018). Additional research is needed to clarify if PB metabolites may also form haptenated proteins, which may promote synergistic interactions resulting in the observed adverse adaptive immune response.

Under normal physiological conditions, the BBB largely restricts entry of peripheral immune cells into the brain, which helps maintain the immune privilege status of the CNS (Van Dyken and Lacoste, 2018). However, peripheral immune cells have been shown to migrate into the brain parenchyma during inflammation resulting from the increases in proinflammatory cytokines and MMP9 activity which weakens the BBB

(Yabluchanskiy et al., 2013; Song et al., 2015; Van Dyken and Lacoste, 2018). We observed elevated proinflammatory cytokines, such as IL-1β and/or TNF-α, in the brains and blood of PB + PER mice (Joshi et al., 2018). Similarly, other studies also support an elevation of proinflammatory cytokines in rodent models of GWI as well as in plasma from veterans with GWI (Khaiboullina et al., 2015; Parkitny et al., 2015; Shetty et al., 2017; Joshi et al., 2018). As such, our observations of increases in these proinflammatory cytokines and in MMP9 and a loss of occludin in PB + PER exposed mice suggests BBB disruptions. Studies on other autoimmune disorders show that autoantibodies against peripheral antigens can enter the brain when the BBB is compromised. Upon entering the brain, they may cross-react with brain proteins, as in the case of SLE where peripherally generated anti-DNA autoantibodies can cross-react with NMDA receptors (Diamond et al., 2009; Brimberg et al., 2015). Hence, a similar mechanism could explain the CNS pathology of GWI, but this requires further investigation.

We also detected 3-PBA-lysine and 3-PBA recovered after protein hydrolysis in the brain. Hence, it is possible that a presence of 3-PBA-protein adducts in the brain could elicit an immune response. While the exact mechanism of how 3-PBA-proteins in the brains of PB + PER mice initiate an immune response is unknown, persistent activation of astroglia suggests that these cells are involved in modulating CNS immune responses following 3-PBA-protein adduct formation. Alternatively, astroglia activation may be secondary to BBB damage as observed in this and other GWI rodent models (Abdel-Rahman et al., 2004; O'Callaghan et al., 2015; Abdullah et al., 2016; Joshi et al., 2018).

Evidence of adaptive immune responses in GWI comes from our observations of increased CCL2 chemokines in the brains of PB + PER exposed mice, which is also reported in other models of GWI (Locker et al., 2017; Shetty et al., 2017). In other autoimmune conditions and in a pesticide-induced mouse model of Parkinson's disease, release of CCL2 by astroglia is shown to promote an ingress of bone-marrow-derived CCR2-expressing monocytes into the brain parenchymal space (Rothhammer and Quintana, 2015; Harrison-Brown et al., 2016; Parillaud et al., 2017). In addition, CX3CR1 is also expressed on bone-marrow derived monocytes whose levels are inversely proportional to both Ly6C and CCR2 in the blood (Jacquelin et al., 2013). We also observed increases in CX3CR1 in the brain homogenates of PB + PER exposed mice. Ligation of this receptor by its ligand CX3CL1 promotes monocyte migration survival and promotes chronic inflammation (O'Sullivan et al., 2016; Parillaud et al., 2017). It is now well-documented that peripheral monocytes are a source of brain macrophages that are distinct from brain-resident microglia, which develop during embryogenesis (Huber et al., 2013; London, Cohen and Schwartz, 2013; Ginhoux and Prinz, 2015). Within this population, tissue-infiltrating monocytes can be further characterized by their expression of Ly6C + ; monocytes positive for this marker are able to migrate into the brain parenchyma and convert into macrophages that are capable of participating in antigen-presentation (Gordon and Taylor, 2005; Jakubzick et al., 2017). These studies collectively suggest an infiltration of monocytes into the CNS after GW pesticide exposure. These data suggest a cross-talk between astroglia and peripheral adaptive immune cells in promoting neuroinflammation, which is further supported by our studies showing activation of NFκB-mediated inflammatory signaling pathways that may be downstream of CCL2-CCR2- and CX3CR1-CX3CL1 ligation, among other pro-inflammatory receptor systems in the brain (Bose and Cho, 2013; Sheridan and Murphy, 2013; Ferretti, Pistoia and Corcione, 2014; Montague et al., 2018). These studies also suggest further examination of these co-stimulatory pathways for the pathogenesis of the CNS pathology of GWI.

5. Conclusions

These explorative studies provide strong evidence that in our PB + PER mouse model of GWI, PER metabolite 3-PBA haptened proteins and promoted adaptive immune responses. We also observe autoantibodies against 3-PBA-haptenated proteins in PB + PER exposed mice and in veterans with GWI. While the exact mechanisms associated with these aberrant autoimmune responses and their effects on the CNS pathology of GWI remain to be elucidated, the work presented herein suggests a cross-talk between the brain immune cells and peripheral adaptive immune cells, which may ultimately promote the entry of peripheral immune cells into the brain and promote neuroinflammatory responses. We anticipate that these studies will help guide future development of biomarkers and therapies for the CNS pathology of GWI.

Declaration of Competing Interest

The author(s) declares no competing interests. The contents do not represent the views of the Department of Veterans Affairs or the United States Government.

Appendix A. Supplementary data

Supplementary data to this article can be found online at https://doi.org/10.1016/j.bbi.2019.07.015.

References

Abdel-Rahman, A., et al., 2004. Stress and combined exposure to low doses of pyridostigmine bromide, DEET, and permethrin produce neurochemical and neuropathological alterations in cerebral cortex, hippocampus, and cerebellum. J. Toxicol. Environ. Health, Part A 67 (2), 163–192. https://doi.org/10.1080/15287390490264802.

Abdullah, L., et al., 2011. Proteomic CNS profile of delayed cognitive impairment in mice exposed to Gulf War agents. NeuroMol. Med. 13 (4), 275–288. https://doi.org/10.1007/s12017-011-8160-z.

Abdullah, L., et al., 2012. Lipidomic profiling of phosphocholine containing brain lipids in mice with sensorimotor deficits and anxiety-like features after exposure to gulf war agents. NeuroMol. Med. 14 (4), 349–361. https://doi.org/10.1007/s12017-012-8192-z.

Abdullah, L., et al., 2016. Translational potential of long-term decreases in mitochondrial lipids in a mouse model of Gulf War Illness. Toxicology 372, 22–33. https://doi.org/10.1016/j.tox.2016.10.012. Elsevier Ireland Ltd.

Abou-Donia, M.B., et al., 2017. Screening for novel central nervous system biomarkers in veterans with Gulf War Illness. Neurotoxicol. Teratol. 61, 36–46. https://doi.org/10.1016/j.ntt.2017.03.002.

Ahn, C. ki, et al., 2007. High-throughput automated luminescent magnetic particle-based immunoassay to monitor human exposure to pyrethroid insecticides. Anal. Chem. https://doi.org/10.1021/ac070675l.

Ahn, K.C., et al., 2011. Immunochemical analysis of 3-phenoxybenzoic acid, a biomarker of forestry worker exposure to pyrethroid insecticides. Anal. Bioanal. Chem. https://doi.org/10.1007/s00216-011-5184-z.

Alberts, B., Johnson, A., Julian, L., 2002. Molecular Biology of the Cell, 4th ed. Garland Science, New York, NY.

Binns, J., et al., 2008. Gulf War Illness and the Health of Gulf War Veterans: Scientific Findings and Recommendations, pp. 1–465.

Bose, S., Cho, J., 2013. Role of chemokine CCL2 and its receptor CCR2 in neurodegenerative diseases. Arch. Pharmacal Res. https://doi.org/10.1007/s12272-013-0161-z.

Brimberg, L., et al., 2015. Antibodies as mediators of brain pathology. Trends Immunol. https://doi.org/10.1016/j.it.2015.09.008.

Broderick, G., et al., 2011. A pilot study of immune network remodeling under challenge in Gulf War Illness. Brain Behav. Immun. 25 (2), 302–313. https://doi.org/10.1016/j.bbi.2010.10.011.

Broderick, G., et al., 2013. Altered immune pathway activity under exercise challenge in Gulf War Illness: an exploratory analysis. Brain Behav. Immun. 28, 159–169. https://

doi.org/10.1016/j.bbi.2012.11.007.

Chao, L.C., et al., 2013. Bone marrow NR4A expression is not a dominant factor in the development of atherosclerosis or macrophage polarization in mice. J. Lipid Res. https://doi.org/10.1194/jlr.M034157.

Craddock, T.J.A., et al., 2015. Achieving remission in Gulf War Illness: a simulation-based approach to treatment design. PLoS ONE 10 (7). https://doi.org/10.1371/journal.pone.0132774.

Diamond, B., et al., 2009. Losing your nerves? Maybe it's the antibodies. Nature Rev. Immunol. https://doi.org/10.1038/nri2529.

Diamond, B., et al., 2013. Brain-reactive antibodies and disease. Annu. Rev. Immunol. https://doi.org/10.1146/annurev-immunol-020711-075041.

Di Domizio, J., Dorta-Estremera, S., Cao, W., 2013. Methylated BSA mimics amyloid-related proteins and triggers inflammation. PLoS ONE. https://doi.org/10.1371/journal.pone.0063214.

Van Dyken, P., Lacoste, B., 2018. Impact of metabolic syndrome on neuroinflammation and the blood-brain barrier. Front. Neurosci. https://doi.org/10.3389/fnins.2018.00930.

Emmerich, T., et al., 2017. Phospholipid profiling of plasma from GW veterans and rodent models to identify potential biomarkers of Gulf War Illness. PLoS ONE 12 (4). https://doi.org/10.1371/journal.pone.0176634.

Ferretti, E., Pistoia, V., Corcione, A., 2014. Role of fractalkine/CX3CL1 and its receptor in the pathogenesis of inflammatory and malignant diseases with emphasis on B cell malignancies. Mediators Inflamm. 2014. https://doi.org/10.1155/2014/480941.

Gangemi, S., et al., 2016. Occupational and environmental exposure to pesticides and cytokine pathways in chronic diseases (Review). Int. J. Mol. Med. https://doi.org/10.3892/ijmm.2016.2728.

Gefen, T., et al., 2015. The effect of haptens on protein-carrier immunogenicity. Immunology. https://doi.org/10.1111/imm.12356.

Gerard, C., Rollins, B.J., 2001. Chemokines and disease. Nat. Immunol. https://doi.org/10.1038/84209.

Ginhoux, F., Prinz, M., 2015. Origin of microglia: current concepts and past controversies. Cold Spring Harbor Perspect. Biol. https://doi.org/10.1101/cshperspect.a020537.

Gordon, S., Taylor, P.R., 2005. Monocyte and macrophage heterogeneity. Nat. Rev. Immunol. https://doi.org/10.1038/nri1733.

Greter, M., Lelios, I., Croxford, A.L., 2015. Microglia versus myeloid cell nomenclature during brain inflammation. Front. Immunol. https://doi.org/10.3389/fimmu.2015.00249.

Grigoryan, H., et al., 2009. Covalent binding of the organophosphorus agent FP-biotin to tyrosine in eight proteins that have no active site serine. Chem. Biol. Interact. https://doi.org/10.1016/j.cbi.2009.03.018.

Han, W., et al., 2015. Cranial irradiation induces transient microglia accumulation, followed by long-lasting inflammation and loss of microglia. Oncotarget. https://doi.org/10.18632/oncotarget.12929.

Harrison-Brown, M., Liu, G.J., Banati, R., 2016. Checkpoints to the brain: directing myeloid cell migration to the central nervous system. Int. J. Mol. Sci. https://doi.org/10.3390/ijms17122030.

Huber, T., et al., 2013. Origin and differentiation of microglia. Front. Cell. Neurosci. https://doi.org/10.3389/fncel.2013.00045.

Ibrahim, S.M., et al., 2018. Activation of α7 nicotinic acetylcholine receptor ameliorates zymosan-induced acute kidney injury in BALB/c mice. Sci. Rep. https://doi.org/10.1038/s41598-018-35254-1.

Jacquelin, S., et al., 2013. CX3CR1 reduces Ly6C high-monocyte motility within and release from the bone marrow after chemotherapy in mice. Blood. https://doi.org/10.1182/blood-2013-01-480749.

Jakubzick, C.V., Randolph, G.J., Henson, P.M., 2017. Monocyte differentiation and antigen-presenting functions. Nat. Rev. Immunol. https://doi.org/10.1038/nri.2017.28.

Jimenez, F., et al., 2010. CCR2 plays a critical role in dendritic cell maturation: possible role of CCL2 and NF-kappa B. J. Immunol. (Baltimore, Md.: 1950) 184 (10), 5571–5581. https://doi.org/10.4049/jimmunol.0803494.

Jokanović, M., 2018. Neurotoxic effects of organophosphorus pesticides and possible association with neurodegenerative diseases in man: a review. Toxicology. https://doi.org/10.1016/j.tox.2018.09.009.

Joshi, U., et al., 2018. Oleoylethanolamide treatment reduces neurobehavioral deficits and brain pathology in a mouse model of Gulf War Illness. Sci. Rep. https://doi.org/10.1038/s41598-018-31242-7.

Karlsson, I., et al., 2018. The fate of a hapten – from the skin to modification of macrophage migration inhibitory factor (MIF) in lymph nodes. Sci. Rep. https://doi.org/10.1038/s41598-018-21327-8.

Khaiboullina, S.F., et al., 2015. Cytokine expression provides clues to the pathophysiology of Gulf War illness and myalgic encephalomyelitis. Cytokine 72 (1), 1–8. https://doi.org/10.1016/j.cyto.2014.11.019.

Koo, B.B., et al., 2018. Corticosterone potentiates DFP-induced neuroinflammation and affects high-order diffusion imaging in a rat model of Gulf War Illness. Brain Behav. Immun. 67, 42–46. https://doi.org/10.1016/j.bbi.2017.08.003.

Lanzavecchia, A., 1985. Antigen-specific interaction between T and B cells. Nature. https://doi.org/10.1038/314537a0.

Lehnardt, S., et al., 2003. Activation of innate immunity in the CNS triggers neurodegeneration through a Toll-like receptor 4-dependent pathway. Proc. National Acad. Sci. https://doi.org/10.1073/pnas.1432609100.

Liebner, S., et al., 2000. Correlation of tight junction morphology with the expression of tight junction proteins in blood-brain barrier endothelial cells. Eur. J. Cell Biol. https://doi.org/10.1078/0171-9335-00101.

Locker, A.R., et al., 2017. Corticosterone primes the neuroinflammatory response to Gulf War Illness-relevant organophosphates independently of acetylcholinesterase inhibition. J. Neurochem. https://doi.org/10.1111/jnc.14071.

London, A., Cohen, M., Schwartz, M., 2013. Microglia and monocyte-derived macrophages: functionally distinct populations that act in concert in CNS plasticity and repair. Front. Cell. Neurosci. https://doi.org/10.3389/fncel.2013.00034.

Macht, V.A., et al., 2018. Pathophysiology in a model of Gulf War Illness: contributions of pyridostigmine bromide and stress. Psychoneuroendocrinology. https://doi.org/10.1016/j.psyneuen.2018.07.015.

Macht, V.A., et al., 2019. Pyridostigmine bromide and stress interact to impact immune function, cholinergic neurochemistry and behavior in a rat model of Gulf War Illness. Brain Behav. Immun. https://doi.org/10.1016/j.bbi.2019.04.015.

Miró-Mur, F., et al., 2016. Immature monocytes recruited to the ischemic mouse brain differentiate into macrophages with features of alternative activation. Brain Behav. Immun. https://doi.org/10.1016/j.bbi.2015.08.010.

Montague, K., et al., 2018. A novel interaction between CX 3 CR 1 and CCR 2 signalling in monocytes constitutes an underlying mechanism for persistent vincristine-induced pain. J. Neuroinflamm. 15, 1. https://doi.org/10.1186/s12974-018-1116-6.

Müller-Mohnssen, H., 1999. Chronic sequelae and irreversible injuries following acute pyrethroid intoxication. Toxicol. Lett. https://doi.org/10.1016/S0378-4274(99)00043-0.

Musilek, K., et al., 2011. Preparation, in vitro screening and molecular modelling of symmetrical 4-tert-butylpyridinium cholinesterase inhibitors – analogues of SAD-128. Bioorg. Med. Chem. Lett. https://doi.org/10.1016/j.bmcl.2010.11.051.

Naisbitt, D.J., et al., 2002. Covalent binding of the nitroso metabolite of sulfamethoxazole leads to toxicity and major histocompatibility complex-restricted antigen presentation. Mol. Pharmacol.

Noort, D., et al., 2008. Protein adduct formation by glucuronide metabolites of permethrin. Chem. Res. Toxicol. https://doi.org/10.1021/tx8000362.

Noort, D., Benschop, H.P., Black, R.M., 2002. Biomonitoring of exposure to chemical warfare agents: a review. Toxicol. Appl. Pharmacol. https://doi.org/10.1016/S0041-008X(02)99449-4.

O'Callaghan, J.P., et al., 2015. Corticosterone primes the neuroinflammatory response to DFP in mice: potential animal model of Gulf War Illness. J. Neurochem. 133 (5), 708–721. https://doi.org/10.1111/jnc.13088.

O'Sullivan, S.A., et al., 2016. Fractalkine shedding is mediated by p38 and the ADAM10 protease under pro-inflammatory conditions in human astrocytes. J. Neuroinflamm. 13 (1), 189. https://doi.org/10.1186/s12974-016-0659-7.

Ochsenbein, A.F., et al., 2000. Protective long-term antibody memory by antigen-driven and T help-dependent differentiation of long-lived memory B cells to short-lived plasma cells independent of secondary lymphoid organs. Proc. Natl. Acad. Sci. https://doi.org/10.1073/pnas.230417497.

Omdal, R., et al., 2005. Neuropsychiatric disturbances in SLE are associated with antibodies against NMDA receptors. Eur. J. Neurol. https://doi.org/10.1111/j.1468-1331.2004.00976.x.

Pakvilai, N., et al., 2014. A Gc-Ecd method for detecting 3-phenoxybenzoic acid in human urine samples and its application in real samples, 8(15), 143–148.

Palm, N.W., Medzhitov, R., 2009. Immunostimulatory activity of haptenated proteins. Proc. Natl. Acad. Sci. https://doi.org/10.1073/pnas.0809403105.

Parihar, V.K., et al., 2013. Mood and memory deficits in a model of Gulf War illness are linked with reduced neurogenesis, partial neuron loss, and mild inflammation in the hippocampus. Neuropsychopharmacology 38 (12), 2348–2362. https://doi.org/10.1038/npp.2013.158.

Parillaud, V.R., et al., 2017. Analysis of monocyte infiltration in MPTP mice reveals that microglial CX3CR1 protects against neurotoxic over-induction of monocyte-attracting CCL2 by astrocytes. J. Neuroinflamm. https://doi.org/10.1186/s12974-017-0830-9.

Parkitny, L., et al., 2015. Evidence for abnormal cytokine expression in Gulf War Illness: a preliminary analysis of daily immune monitoring data. BMC Immunol. 16, 57. https://doi.org/10.1186/s12865-015-0122-z.

Proudfoot, A.T., 2005. Poisoning due to pyrethrins. Toxicol. Rev. https://doi.org/10.2165/00139709-200524020-00004.

Qiang, L., et al., 2017. Reprogramming cells from Gulf War veterans into neurons to study Gulf War illness. Neurology 88 (20), 1968–1975. https://doi.org/10.1212/WNL.0000000000003938.

Randolph, G.J., Jakubzick, C., Qu, C., 2008. Antigen presentation by monocytes and monocyte-derived cells. Curr. Opin. Immunol. https://doi.org/10.1016/j.coi.2007.10.010.

Rothhammer, V., Quintana, F.J., 2015. Control of autoimmune CNS inflammation by astrocytes. Seminars Immunopathol. https://doi.org/10.1007/s00281-015-0515-3.

Santer, D.M., et al., 2013. Enhanced activation of memory, but not naïve, B cells in chronic hepatitis C virus-infected patients with cryoglobulinemia and advanced liver fibrosis. PLoS ONE. https://doi.org/10.1371/journal.pone.0068308.

Schactae, A.L., et al., 2017. Congenital muscular dystrophy 1D causes matrix metalloproteinase activation and blood-brain barrier impairment. Curr. Neurovasc. Res. https://doi.org/10.2174/1567202613666161201204549.

Sheridan, G.K., Murphy, K.J., 2013. Neuron-glia crosstalk in health and disease: fractalkine and CX3CR1 take centre stage. Open Biol. 3 (12), 130181. https://doi.org/10.1098/rsob.130181.

Shetty, G.A., et al., 2017. Chronic oxidative stress, mitochondrial dysfunction, Nrf2 activation and inflammation in the hippocampus accompany heightened systemic inflammation and oxidative stress in an animal model of gulf War Illness. Front. Mol. Neurosci. https://doi.org/10.3389/fnmol.2017.00182.

Song, J., et al., 2015. Focal MMP-2 and MMP-9 activity at the blood-brain barrier promotes chemokine-induced leukocyte migration. Cell Rep. https://doi.org/10.1016/j.celrep.2015.01.037.

Steele, 2000. Prevalence and patterns of Gulf War illness in Kansas veterans: association of symptoms with characteristics of person, place, and time of military service. Am. J. Epidemiol. https://doi.org/10.1093/aje/152.10.992.

Stern, J.N.H., et al., 2014. B cells populating the multiple sclerosis brain mature in the

draining cervical lymph nodes. Sci. Transl. Med. https://doi.org/10.1126/scitranslmed.3008879.

Sullivan, K., et al., 2018. Neuropsychological functioning in military pesticide applicators from the Gulf War: effects on information processing speed, attention and visual memory. Neurotoxicol. Teratol. https://doi.org/10.1016/j.ntt.2017.11.002.

Tailor, A., et al., 2016. Mass spectrometric and functional aspects of drug-protein conjugation. Chem. Res. Toxicol. https://doi.org/10.1021/acs.chemrestox.6b00147.

Thiphom, S., et al., 2012. An enzyme-linked immunosorbent assay for detecting 3-phenoxybenzoic acid in plasma and its application to farmers and consumers. Anal. Methods. https://doi.org/10.1039/c2ay25642h.

Thrasher, J.D., Madison, R., Brouchton, A., 1993. Immunologic abnormalities in humans exposed to chlorpyrifos: preliminary observations. Arch. Environ. Health. https://doi.org/10.1080/00039896.1993.9938400.

Tracey, K.J., 2005. Fat meets the cholinergic antiinflammatory pathway: figure 1. J. Exp. Med. https://doi.org/10.1084/jem.20051760.

Underly, R.G., et al., 2016. Pericytes as inducers of rapid, matrix metalloproteinase-9-dependent capillary damage during ischemia. J. Neurosci. https://doi.org/10.1523/jneurosci.2891-16.2016.

Vaure, C., Liu, Y., 2014. A comparative review of toll-like receptor 4 expression and functionality in different animal species. Front. Immunol. https://doi.org/10.3389/fimmu.2014.00316.

Vojdani, A., Thrasher, J.D., 2004. Cellular and humoral immune abnormalities in Gulf War veterans. Environ. Health Perspect. 112 (8), 840–846. https://doi.org/10.1289/ehp.6881.

Warrington, R., 2012. Drug allergy: causes and desensitization. Human Vaccines and Immunotherapeutics. https://doi.org/10.4161/hv.21889.

White, R.F., et al., 2016. Recent research on Gulf War illness and other health problems in veterans of the 1991 Gulf War: Effects of toxicant exposures during deployment. Cortex 449–475. https://doi.org/10.1016/j.cortex.2015.08.022.

Winkenwerder, W., 2003. Environmental Exposure Report: Pesticides Final Report. U.S. Department of Defense, Office of the Special Assistant to the Undersecretary of Defense (Personnel and Readiness) for Gulf War Illnesses Medical Readiness and Military Deployments, Washington, D.C.

Wohleb, E.S., et al., 2013. Stress-induced recruitment of bone marrow-derived monocytes to the brain promotes anxiety-like behavior. J. Neurosci. https://doi.org/10.1523/jneurosci.1671-13.2013.

Wong, M., et al., 2017. Abnormal microglia and enhanced inflammation-related gene transcription in mice with conditional deletion of Ctcf in Camk2a-Cre-expressing neurons. J. Neurosci. https://doi.org/10.1523/jneurosci.0936-17.2017.

Yabluchanskiy, A., et al., 2013. Matrix metalloproteinase-9: many shades of function in cardiovascular disease. Physiology. https://doi.org/10.1152/physiol.00029.2013.

Yang, S., et al., 2017. Identification of two immortalized cell lines, ECV304 and bEnd3, for in vitro permeability studies of blood-brain barrier. PLoS ONE. https://doi.org/10.1371/journal.pone.0187017.

Zakirova, Z., et al., 2015. Gulf War agent exposure causes impairment of long-term memory formation and neuropathological changes in a mouse model of Gulf War Illness. PLoS ONE 10 (3). https://doi.org/10.1371/journal.pone.0119579.

Zarruk, J.G., Greenhalgh, A.D., David, S., 2018. Microglia and macrophages differ in their inflammatory profile after permanent brain ischemia. Exp. Neurol. https://doi.org/10.1016/j.expneurol.2017.08.011.

Zhou, T., et al., 2017. Microglia polarization with M1/M2 phenotype changes in rd1 mouse model of retinal degeneration. Front. Neuroanat. https://doi.org/10.3389/fnana.2017.00077.